NASA TECHNICAL NOTE

NASA TN D-2644

NASA TN D-2644

PROPAGATION OF CYLINDRICAL AND SPHERICAL ELASTIC WAVES BY METHOD OF CHARACTERISTICS

by Pei Chi Chou and Herbert Abraham Koenig

Prepared under Grant No. NsG-270-63 *by*
DREXEL INSTITUTE OF TECHNOLOGY
Philadelphia, Pa.
for

NATIONAL AERONAUTICS AND SPACE ADMINISTRATION • WASHINGTON, D. C. • FEBRUARY 1965

ERRATA

NASA Technical Note D-2644

PROPAGATION OF CYLINDRICAL AND SPHERICAL ELASTIC WAVES BY METHOD OF CHARACTERISTICS

by

Pei Chi Chou

Herbert Abraham Koenig

January 7, 1966

Pages 26-48 (Excluding pages 32-33): The abscissa scale on these graphs is incorrectly given as 3, 6, 9, etc. To correct the scale, multiply each of the abscissa values by 0.934, i.e., change 3 to 2.8.

Pages 32-33: The abscissa scale on these two graphs is incorrectly given as 3, 6, 9, etc. To correct the scale, multiply each of the abscissa values by 0.429, i.e., change 3 to 1.287.

Page 40: On the $\bar{r} = 2.016$ curve, the maximum value for radial stress should be 0.486 instead of 0.617.

Page 46: On the $\bar{r} = 2.016$ curve, the maximum value for radial stress should be 0.486 instead of 0.617 and the minimum value should be -0.442 instead of -0.562.

Page 56: Equation (A.23) should read $\epsilon_\theta = \frac{u}{r}$

Page 58: Equation (A.31) should read $C = C_2 = \sqrt{\frac{E_2}{\rho}} = \sqrt{\frac{E_0(1-\nu_0)}{\rho(1-\nu_0-2\nu_0^2)}}$

Pages 62 and 63: Equations (B.3) and (B.6) should read:

$$= \frac{1}{\frac{1-M}{E}(dr)^3\left(\frac{dt}{dr}+\frac{1}{C}\right)\left(\frac{dt}{dr}-\frac{1}{C}\right)}\cdot\left\langle\frac{1}{E}(dr)^2\left\{M\frac{dt}{dr}\left[N(\sigma_\theta-\sigma_r)dt+\rho r\,dv\right]-\rho r\left[\frac{1}{E}d\sigma_r(M-N\nu^2)-N\nu\frac{v}{r}dt\right]\right\}\right\rangle \tag{B.3}$$

$$\frac{d\sigma_\theta}{dr} = \frac{1}{\frac{1-M}{E}(dr)^3\left(\frac{dt}{dr}+\frac{1}{C}\right)\left(\frac{dt}{dr}-\frac{1}{C}\right)}\left\{-r\left[\frac{\nu}{E}d\sigma_r-\frac{M}{E}d\sigma_\theta+\frac{v}{r}dt\right]+\frac{\nu}{E}\left(\frac{dr}{dt}\right)\left[N(\sigma_\theta-\sigma_r)dt+\rho r\,dv\right]+\rho r\left(\frac{dr}{dt}\right)^2\left[\frac{v}{Er}dt+N\left(\frac{\nu}{E}\right)^2d\sigma_\theta-\frac{M}{E^2}d\sigma_\theta\right]\right\} \tag{B.6}$$

Issued 6-10-66

PROPAGATION OF CYLINDRICAL AND SPHERICAL ELASTIC WAVES BY METHOD OF CHARACTERISTICS

By Pei Chi Chou and Herbert Abraham Koenig

Prepared under Grant No. NsG-270-63 by
DREXEL INSTITUTE OF TECHNOLOGY
Philadelphia, Pa.

for

NATIONAL AERONAUTICS AND SPACE ADMINISTRATION

For sale by the Office of Technical Services, Department of Commerce,
Washington, D.C. 20230 -- Price $3.00

TABLE OF CONTENTS

PROPAGATION OF CYLINDRICAL AND SPHERICAL ELASTIC WAVES BY METHOD OF CHARACTERISTICS

by Pei Chi Chou and Herbert Abraham Koenig

Drexel Institute of Technology
Philadelphia, Pa.

SUMMARY

A set of generalized equations is presented which governs the propagation of plane, cylindrical and spherical dilatation waves in elastic media. The corresponding characteristic equations are then derived, including the propagation of abrupt changes (discontinuous wave fronts). Procedures of numerical integration along the characteristic directions are established and carried out for several examples on an electronic computer. The solutions of four of the specific examples calculated show excellent agreement with existing solutions by other methods. Certain interesting phenomena have been discussed which may have considerable significance in dynamic crack propagation and dynamic strength of materials.

SYMBOLS

c = wave speed

c_o = bar velocity = $\sqrt{E_o/\rho}$

c_2 = dilatational velocity = $\sqrt{E_o(1-\nu_o)/[\rho(1+\nu_o)(1-2\nu_o)]}$

c_p = plate velocity $\simeq$ $\sqrt{E_o/\rho(1-\nu_o^2)}$

E_o = Modulus of Elasticity

E_1 = $E_o/(1 - \nu_o^2)$

E_2 = $E_o(1 - \nu_o)/(1 - \nu_o - 2\nu_o^2)$

K = arbitrary constant

k = time for a ramp input to reach its maximum value

N = constant which determines nature of problem

p_o = initial pressure at hole

r = radial distance

r_o = inner radius of solid

$\bar{r}$ = r/r_o

t = time

u = radial displacement

v = $\partial u/\partial t$ = particle velocity

$\bar{v}$ = v/c

α = modifying constant

ν_o = Poisson's ratio

ν_1 = $\nu_o/(1 - \nu_o)$

σ_r = radial stress

σ_θ = tangential stress

$\bar{\sigma}$ = σ/E

τ = ct/r_o

ρ = density

I. INTRODUCTION

Recently, considerable interest has been centered on the protection of the fuel tank and other parts of a space vehicle against meteoroid impact. The structural walls of space vehicles are subject to the hazard of meteoroid penetration. In addition, the wall of the fuel tank must be able to withstand the high pressure created by a high speed projectile after entering the tank. From an analytical point of view, these problems can be treated as a thin plate with a hole subjected to dynamic loading at the edge of the hole.

The theoretical analysis of transient stresses due to impact loadings has generally been performed by a mode-superposition method that uses the natural modes of vibration predicted by elementary theory. For very sharp impact loadings, however, this approach is not satisfactory because many modes are often required for convergence. A natural alternative to the modal method of calculating transient stresses is the method of characteristics. Although this method has been successfully used to treat such simple problems as longitudinal and torsional impact of rods, only recently have serious attempts been made to study the transient response of more complicated structures by this approach. Leonard and Budiansky [1] derived the characteristic equations for the Timoshenko beam, including transverse shear effect and rotary inertia. They also derived the equations governing the propagation of discontinuities and performed numerical integration along the characteristics for a few specific examples. Following the same general approach, Jahsman [2] derived

the characteristic equations for circular sheets and plates under very general loading conditions at an inner hole. He obtained the relations between the various stresses at the wave fronts due to abrupt inputs (step inputs), but did not solve the characteristic equations for the distribution of stresses behind the fronts.

In this report, the problem of a circular sheet under dynamic-in-plane loading at an inner hole is solved by the method of characteristics. There are two purposes for solving this problem; first, we are interested in developing the method of characteristics so that it may be applied later to other more complicated plate equations including the effects of bending, stretching, and shearing. Second, the solution obtained in this report for sheets under in-plane loading has direct engineering applications. The governing equations for the sheet problems are of the same general form as those for plane strain problems and for spherical symmetrical problems. Although different techniques are involved in solving these three types of problems by the Laplace transform method, they can be treated by the same approach in the method of characteristics. In this report, therefore, a set of generalized equations is formulated which is applicable to plane waves, cylindrical waves (plane stress or plane strain), and spherical waves. A few specific examples of sheets and spheres under various inputs are solved by the method of characteristics.

The problem of a circular sheet under a suddenly applied radial stress at an inner hole was solved by Kromm [3], using the Laplace transform method. In a subsequent paper [4], by using the same approach, he also solved the problem of a sheet under a step velocity

input. Miklowitz [5] obtained a solution for a ramp radial stress input by the Laplace transform method with a different inversion technique. The corresponding plane strain problem for a thick wall cylinder was analyzed by Selberg [6]. In these four cases of plane stress and plane strain problems, the solutions are in the form of integrals which must be evaluated by either infinite series or by approximate numerical integration. For a different input function, another lengthy transform and inversion process must be carried out and the resulting integral evaluated separately by numerical means. Thus the Laplace transform method applied to cylindrical dilatational wave problems can only produce approximate numerical results and is not convenient for systematic study of the effects due to various input functions. On the other hand, the method of characteristics, although numerical in nature, as will be shown in this report, is very simple and easy to apply, and suitable for problems of any type of input functions.

For the problem of spherical dilatational waves in hollow spheres, closed form analytical solutions exist. The classical theory and the general solution for spherical elastic waves are treated in textbooks such as Kolsky [7]. Hopkins [8] formulated the characteristic equations for spherical elastic and plastic waves, including shock waves in the plastic region, but did not carry out the solution for any specific problem. Sharpe [9] obtained analytical closed form solutions for both an exponential pressure input and a step pressure input. Allen and Goldsmith [10] carried out extensive numerical calculations for the solution of the exponential input by Sharpe. The same problem is treated in this report by the method of

characteristics and numerical results almost identical to those of Allen and Goldsmith are obtained.

For practical spherical wave problems such as those due to underground explosions and due to hypervelocity impacts, the inputs are usually irregular functions and must be expanded into infinite series form before the closed form analytical solution for simple input functions can be used, as discussed by Kinslow [11]. For these problems, the numerical method of characteristics is again more convenient.

It has just come to the authors' attention that very recently (1964) in Poland, Perzyna and Bejda [12] applied the method of characteristics to spherical stress waves in plastic medium; and Kaliski, Nowacki, and Wlodarczyk [13] used the same method in treating propagation and reflection of a spherical wave in an elastic-visco-plastic strain-hardening body. They followed in general the approach discussed by Hopkins [8].

In the following pages, the unified equations for plane, cylindrical, and spherical elastic waves are presented. The characteristic equations are then derived, including the relations governing the propagation of discontinuities. Specific examples with various input functions are then solved by integrating along the characteristic lines. The calculations are performed on an electronic computer. For the few examples where solutions by other methods exist, our results are in excellent agreement with solutions by other techniques. Because of the simplicity of the present method, solutions for many inputs are calculated. From these solutions, many interesting phenomina have been discovered.

Currently, this method is being extended to media with variable elastic properties and exterior boundaries. It is also being applied to the plate bending problem.

II. Governing Equations

One-dimensional elastic dilatational waves, including plane, cylindrical and spherical waves, can be analyzed by one set of generalized equations. As derived in Appendix A, these equations are

$$\frac{\partial \sigma_r}{\partial r} + \frac{N(\sigma_r - \sigma_\theta)}{r} = \rho \frac{\partial^2 u}{\partial t^2} \tag{1}$$

$$\frac{\partial u}{\partial r} = \frac{1}{E}\left(\sigma_r - N\nu\sigma_\theta\right) \tag{2}$$

$$N\frac{u}{r} = \frac{N}{E}\left\{\sigma_\theta\left[1 - (N-1)\nu\right] - \nu\sigma_r\right\} \tag{3}$$

where r is the coordinate and u the displacement, both in the direction of the wave propagation; t is time; ρ is density; σ_r and σ_θ are the normal stresses on planes parallel and normal to the wave front, respectively; E and ν are generalized elastic constants to be defined below. In these equations, N is a constant, with values of zero, one, and two, corresponding to the plane, cylindrical and spherical waves, respectively. For plane waves, N = 0, ν vanishes from eqs. (1), (2), and (3), but E can assume three different values depending on the geometry of the medium:

$$E = E_0 = \text{Modulus of Elasticity} \quad \text{for bars} \tag{4}$$

$$E = E_1 = \frac{E_0}{1 - \nu_0^2} \quad \text{for sheets} \tag{5}$$

$$E = E_2 = \frac{E_0(1-\nu_0)}{1 - \nu_0 - 2\nu_0^2} \quad \text{for infinite bodies} \tag{6}$$

where ν_0 is the Poisson's ratio. For cylindrical waves, N = 1, the constants E and ν can assume two sets of values depending on the geometry of the problem:

$$\left.\begin{aligned} E &= E_o \\ \nu &= \nu_o \end{aligned}\right\} \quad \text{For sheets (plane stress)} \tag{7}$$

$$\left.\begin{aligned} E &= E_1 \\ \nu &= \nu_1 = \frac{\nu_o}{1-\nu_o} \end{aligned}\right\} \quad \text{For infinite bodies (plane strain)} \tag{8}$$

Spherical waves can only exist in infinite bodies; thus we have for N = 2 only one set of values for E and ν,

$$\left.\begin{aligned} E &= E_o \\ \nu &= \nu_o \end{aligned}\right\} \quad \text{For infinite bodies} \tag{9}$$

Eliminating σ_r and σ_θ from eqs. (1), (2), and (3), we obtain

$$\frac{\partial^2 u}{\partial r^2} + N \frac{\partial}{\partial r}\left(\frac{u}{r}\right) = \frac{1}{C^2}\frac{\partial^2 u}{\partial t^2} \tag{10}$$

which is the governing differential equation in terms of u. The values of c, the wave propagation velocity, for various cases, are

$$c = c_o = \sqrt{\frac{E_o}{\rho}} = \text{bar velocity--for plane waves in bars} \tag{11}$$

$$c = c_p = \sqrt{\frac{E_o}{\rho(1-\nu_o^2)}} = \text{plate velocity--for plane and cylindrical waves in sheets} \tag{12}$$

$$c = c_2 = \sqrt{\frac{E_o(1-\nu_o)}{\rho(1-\nu_o-2\nu_o^2)}} = \text{dilatational velocity--for plane, cylindrical and spherical waves in infinite bodies} \tag{13}$$

For plane waves, the general solution of eq. (10) is the familiar d'Alembert's solution involving waves of constant amplitude. Hence, only cylindrical and spherical waves will be considered below.

Eq. (10), which is a second order differential equation with one dependent variable u, is equivalent to the system of eqs. (1), (2), and (3). Eq. (10) is more convenient for the application of the Laplace transform method [3]. For the method of characteristics, it is advantageous to use the system of eqs. (1) to (3), because the expressions for the boundary conditions are simpler when the dependent variables are σ_r, σ_θ, and $\partial u/\partial t$. Differentiating eqs. (2) and (3) with respect to time, and letting $v = \partial u/\partial t$, we have the system of equations

$$\frac{\partial \sigma_r}{\partial r} + \frac{N(\sigma_r - \sigma_\theta)}{r} = \rho \frac{\partial v}{\partial t} \tag{14}$$

$$\frac{\partial v}{\partial r} = \frac{1}{E}\left(\frac{\partial \sigma_r}{\partial t} - N\nu \frac{\partial \sigma_\theta}{\partial t}\right) \tag{15}$$

$$\frac{v}{r} = \frac{1}{E}\left\{\frac{\partial \sigma_\theta}{\partial t}\left[1 - (N-1)\nu\right] - \nu \frac{\partial \sigma_r}{\partial t}\right\} \tag{16}$$

This is a system of three linear first-order partial differential equations with σ_r, σ_θ, and v as the dependent variables. These equations will be shown to be hyperbolic and the corresponding characteristic equations will be presented in the next section.

III. Method of Characteristics

A. Characteristic Equations

In the r,t-plane, certain curves might exist, along which the stresses and velocity are continuous, but the derivatives of σ_r, σ_θ, and v are discontinuous. These curves will be called the physical characteristics, (or simply, characteristics, or waves) and the relation governing the variation of σ_r, σ_θ, and v along these physical characteristics will be called characteristic equations, which are usually called the hodograph characteristics in gas dynamics. As shown in Appendix B, for the system of eqs. (14), (15), and (16), the physical characteristics are

$$\begin{aligned} I^+ \qquad & \frac{dr}{dt} = +c \\ I^- \qquad & \frac{dr}{dt} = -c \\ II \qquad & dr = 0 \end{aligned} \tag{17}$$

The I^+ characteristic represents propagation of the discontinuity in the derivatives at velocity c, traveling to the right in the r,t-plane. The I^- characteristic gives the propagation towards the left, while II is a degenerate dynamic wave expressing conditions along lines with r = constant. For homogeneous materials of constant E and ν_o, the velocity of propagation c is constant throughout the medium and the physical characteristics are straight lines of constant slope.

The characteristic equations along I^+ and I^- are, respectively,

$$d\sigma_r \mp \rho c\, dv = \left\{ -N(\sigma_r - \sigma_\theta) \pm \rho \nu c v \left[\frac{N}{1-(N-1)\nu} \right] \right\} \frac{dr}{r} \tag{18}$$

The characteristic equation along II is

$$\frac{d\sigma_r}{d\sigma_\theta} = \left\{ \left[1 - (N-1)\nu \right] - \frac{Ev}{r} \frac{dt}{d\sigma_\theta} \right\} \frac{1}{\nu} \tag{19}$$

Eq. (19) is merely a restatement of eq. (16), which gives the static relation between the differentials of stresses and velocity at any constant r.

B. Propagation of Discontinuity

The characteristic eqs. (18) and (19) are applicable for continuous fields with possible discontinuity in the derivatives of the variables σ_r, σ_θ, and v. Across the physical characteristics, discontinuities in the variables themself may also exist, but these will not be governed by eqs. (18) or (19). Discontinuity in σ_r, σ_θ, and v occurs when a finite step input (or jump input) in these variables is applied at a particular r. The equations governing the propagation of these discontinuities will be derived below following the general procedure given by Leonard and Budiansky [1] and Jahsman [2].

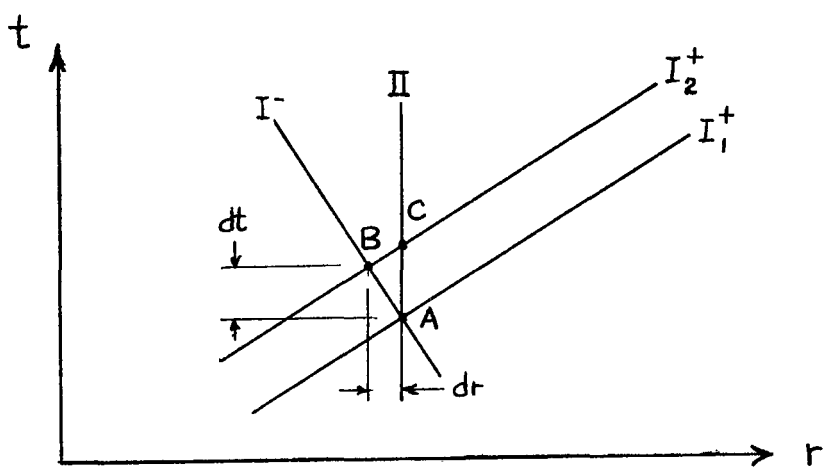

Figure 1 Discontinuities Propagating Along A I^+ Characteristic

Let A and B be two points on a I^- characteristic as shown in Fig. 1. The two I^+ characteristics passing through A and B are represented by I_1^+, and I_2^+ respectively. If a discontinuity of σ_r across I_1^+ exists, then $\sigma_{rB} - \sigma_{rA} = \delta\sigma_r$ is finite but different from zero as I_2^+ is allowed to approach I_1^+, or as dr approaches zero. Writing eq. (18) (with the lower sign, for I^-) and integrating from A to B, we have

$$(\sigma_{rB} - \sigma_{rA}) + \rho c (v_B - v_A) = \int_A^B \left\{ -N(\sigma_r - \sigma_\theta) - \nu\rho c v \left[\frac{N}{1-(N-1)\nu} \right] \right\} \frac{dr}{r}$$

or

$$\delta\sigma_r + \rho c \, \delta v = 0 \tag{20}$$

since when $dr \to 0$, the integrand contains bounded values of σ_r, σ_θ, and v, so that the right-hand side vanishes. Similarly, integration along II from I_1^+ to I_2^+ (or from A to C) yields

$$\delta\sigma_r = \frac{1}{\nu}\left[1 - (N-1)\nu \right] \delta\sigma_\theta \tag{21}$$

where

$$\delta\sigma_r = \sigma_{rC} - \sigma_{rA} \quad \text{and} \quad \delta\sigma_\theta = \sigma_{\theta C} - \sigma_{\theta A}$$

Since the variations in σ_r and σ_θ along I_2^+ are continuous, as I_2^+ approaches I_1^+, and C approaches A and B, we have

$$\lim_{dt \to 0} (\sigma_{rC} - \sigma_{rA}) = \lim_{dt \to 0} (\sigma_{rB} - \sigma_{rA}), \text{ etc.} \tag{22}$$

Therefore, the value of $\delta\sigma_r$ in eq. (21) approaches the $\delta\sigma_r$ in eq. (20), and represents the jump in σ_r at point A across I_1^+. The same is true for $\delta\sigma_\theta$ and δv.

The variation in amplitude of the functions $\delta\sigma_r$, $\delta\sigma_\theta$ and δv as they propagate along I^+ is obtained by writing eq. (18), with the

upper sign, along I_2^+ and I_1^+, and subtracting one from the other. As $dr \to 0$, we have

$$d(\delta\sigma_r) - \rho c\, d(\delta v) = \left\{ -N(\delta\sigma_r - \delta\sigma_\theta) + \nu\rho c\, \delta v \left[\frac{N}{1-(N-1)\nu} \right] \right\} \frac{dr}{r} \tag{23}$$

Eliminating $\delta\sigma_\theta$ and δv by eqs. (20) and (21), yields

$$\frac{d(\delta\sigma_r)}{d\sigma_r} = -\frac{N}{2}\frac{dr}{r} \tag{24}$$

This may be integrated to give

$$\delta\sigma_r = K r^{-N/2} \tag{25}$$

where K is a constant. Substitution of this into eqs. (20) and (21) then furnishes the equations for the variation of $\delta\sigma_\theta$ and δv. Following the same procedure, the equations for discontinuities across a I^- characteristic can also be derived. Therefore, for discontinuities across I^+ and I^- characteristics, we have

$$\delta\sigma_r = K r^{-N/2} \tag{25}$$

$$\delta\sigma_\theta = \left[\frac{\nu}{1-(N-1)\nu} \right] K r^{-N/2} \tag{26}$$

$$\delta v = \mp \frac{1}{\rho c} K r^{-N/2} \tag{27}$$

From these, it may be seen that discontinuities or abrupt changes across cylindrical waves (N = 1) vary as $r^{-1/2}$ when they propagate inward or outward. This is in agreement with Kromm [4] and Jahsman [2] for the case of sheets. For spherical waves, discontinuities vary as r^{-1}, in agreement with the classical theory, [7] [8].

C. Initial and Boundary Conditions

In this paper, the elastic body under consideration will be either an infinite sheet with a circular hole, or an infinite hollow cylinder, or an infinite hollow sphere. These configurations can be represented by $r_o \leq r < \infty$, where r_o is a constant. Initially, the body is not loaded, thus the stress and velocity are zero. As time progresses, the input is applied at $r = r_o$, either suddenly or gradually. This input can be in the form of specified time function of any one of three variables, σ_r, σ_θ, and v, at $r = r_o$. In actual cases, the application of σ_θ load is not practical. Thus in the following sections several types of input in terms of σ_r and v are presented.

IV. Numerical Procedures

A numerical procedure involving stepwise integration along the characteristics is employed to solve problems of various inputs. In the r,ct-plane, the region between $r = r_o$ and $r = r_o + ct$ is divided into a grid system by the three physical characteristics. The properties at each grid point will be calculated; thus, the continuous domain is replaced by discrete points.

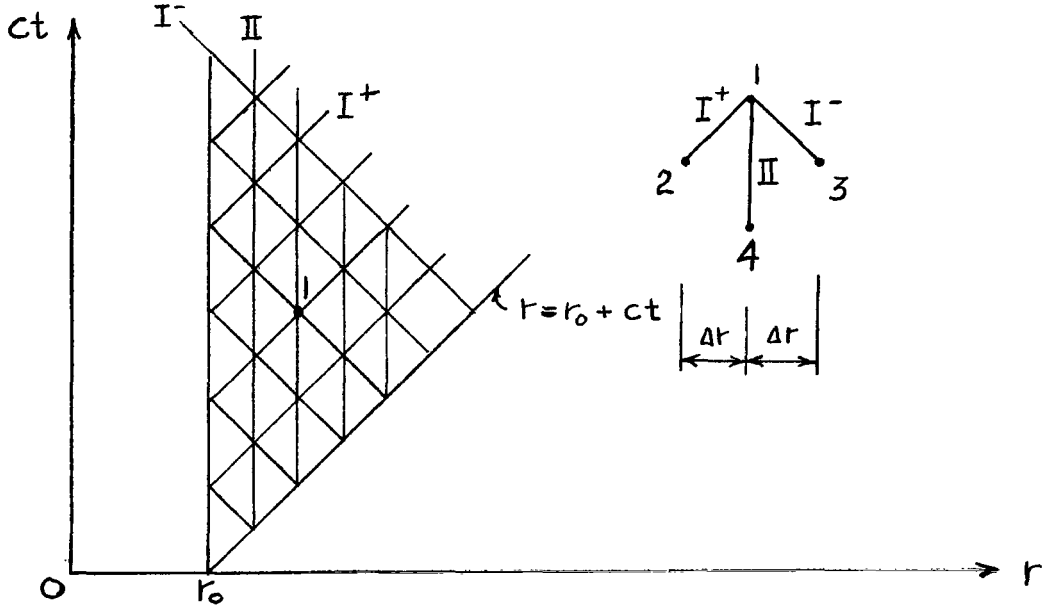

Figure 2 Characteristic Network for Application of Numerical Procedure

At a typical interior point 1, the three quantities σ_r, σ_θ, and v can be calculated, if all the stresses and velocities at three neighboring points 2, 3, and 4 are known. Between points 1 and 2, along a I^+ characteristic, eq. (18) with the upper sign is written in finite-difference form. Along I^- from points 3 to 1 and along II from 4 to 1, the corresponding characteristic equations are also expressed in finite-difference algebraic form. The three unknowns σ_r, σ_θ, and v at point 1 can then be determined from these three equations.

Along the line $r = r_o$, where one of the three variables is prescribed, the remaining two variables may be determined from the two equations along the I^- and II characteristics. In the region $r > r_o + ct$, the stresses and velocity are zero. Along the line $r = r_o + ct$, the stresses and velocity are also zero if the initial input at $r = r_o$ is continuous (rather than a step input). If, however, a discontinuous input (step input) is applied at $r = r_o$ and $t = 0$, the values of σ_r, σ_θ, and v are different from zero along $r = r_o + ct$ and may be determined from eqs. (25), (26), and (27).

V. Specific Examples

A few specific examples of sheets and spheres under various inputs at $r = r_o$ are calculated and presented below. Results of some of these examples will be compared with existing solutions by other methods.

In presenting the results, nondimensional quantities are introduced as follows:

$$\bar{r} = r/r_o \,, \quad \tau = tc/r_o \,, \quad \bar{\sigma} = \sigma/E \,, \quad \bar{v} = v/c$$

Thus, the results are true for materials of any values of E_o and ρ and for any value of r_o. In all examples (except case I) 0.3 is used for ν_o. For the sheets ($N = 1$, $E = E_o$, $\nu = \nu_o$), the examples include a) a step function in σ_r, b) ramp functions in σ_r, c) a rectangular function (impulsive) in σ_r and d) a step function in v. For spherical cases ($N = 2$), in addition to the step, ramp, and rectangular inputs in σ_r and step and ramp inputs in v, an exponential input in σ_r is also calculated and compared with an analytical closed form solution.

A. Step $\bar{\sigma}_r$ Input in Sheets

This problem has been solved by Kromm [3] using the Laplace transform method. Within the accuracy of curve plotting, our results for a unit step $\bar{\sigma}_r$ input, as shown in Fig. 3, agree exactly with Kromm's. Figs. 3a, 3b, and 3c give the distributions of $\bar{\sigma}_r$, $\bar{\sigma}_\theta$, and v, respectively, all plotted against τ, with $\bar{r}$ as a parameter. The abrupt wave fronts in $\bar{\sigma}_r$, $\bar{\sigma}_\theta$, and $\bar{v}$ propagate outward at a velocity c_p. The amplitude of these wave fronts attenuate according to eqs. (25), (26), and (27). At large values of time,

the velocities at all radii approach zero and the stresses approach their static values. Other properties of these curves have been discussed by Kromm. An additional interesting point concerning the behavior of σ_θ at the hole ($\bar{r} = 1$) may be mentioned. Immediately after the application of the step $\bar{\sigma}_r$ input, $\bar{\sigma}_\theta$ becomes $\nu_o \bar{\sigma}_r$ (0.3 in this case). After a short time ($\tau = 3.88$; or $t = 4.75\mu$sec. for $\rho = .000793 \frac{lb\text{-}sec^2}{in^4}$, $r_o = 0.25$ in., $E_o = 30 \times 10^6$ psi) $\bar{\sigma}_\theta$ decreases to a value of -1.24, and then increases again to its static value of -1. This initial positive value of $\bar{\sigma}_\theta$ and subsequent surge to a high negative value have important implications in crack propagation and in dynamic strength of materials.

B. Ramp $\bar{\sigma}_r$ Inputs in Sheets

This is the exact problem of Miklowitz [5], who applied the Laplace transform method in getting a solution. As mentioned before, his solution is in the form of a lengthy quadrature which must be evaluated by approximate numerical methods. Our results by the method of characteristics, as shown in Fig. 4, are identical to his results in graphical form. The slope of the ramp is taken as $\bar{k} = 2.04$ which is equivalent to a "k" of 2.5μsec., for $r_o = .25$ in. and $E_o = 30 \times 10^6$ psi, (which are the values used in [5]). From Fig. 4 it can be seen that the initial positive value of $\bar{\sigma}_\theta$ is less than $\nu_o \bar{\sigma}_r$, the value for step input. The subsequent downward surge in $\bar{\sigma}_\theta$ is also less than that due to the step input. The wave front still propagates at a velocity of c_p, but the stresses and velocity increase gradually after the arrival of the front. At large values of time, velocities at all radii become zero and the stresses approach

the static values for $\bar{\sigma}_r = 1$ at $\bar{r} = 1$. To bring out some further features of the response of a sheet to ramp inputs, a few cases using different values of $\bar{k}$ are calculated and the results plotted in Fig. 5. As the ramp becomes steeper ($\bar{k}$ decreasing), the solution approaches that of a step input as a limit.

From a practical point of view, most inputs are gradually applied. Also, since a step input always involves short length waves from the normal mode point of view, the plane stress approximation is therefore not accurate. However, since the dynamic stresses due to the step input are larger than those due to ramp inputs (or other gradually applied inputs), solutions for the step input may be used to establish upper bounds of dynamic responses to different loading functions.

C. A Rectangular $\bar{\sigma}_r$ Input in Sheets

The fact that, due to a step $\bar{\sigma}_r$ input, the peak $\bar{\sigma}_\theta$ at $\bar{r} = 1$ is 24 percent higher than the static value has been recognized by Kromm. (For a ramp $\bar{\sigma}_r$ input with $\bar{k} = 2.04$, the peak is 23 percent higher, as shown in Fig. 4b) We shall bring out another interesting and important fact about $\bar{\sigma}_r$ input functions. This is the case of a rectangular $\bar{\sigma}_r$ input, or a unit step $\bar{\sigma}_r$ input at $\tau = 0$ combined with a negative unit step $\bar{\sigma}_r$ input at $\tau = 3.88$. As shown in Fig. 6, this is equivalent to an impulsive input involving a loading and unloading process. Due to the initial positive value and then a negative surge of $\bar{\sigma}_\theta$ under the step $\bar{\sigma}_r$ input, the peak $\bar{\sigma}_\theta$ under the rectangular input is 54 percent higher than the static value due to $\bar{\sigma}_r = 1$ at $\bar{r} = 1$, as shown in Fig. 6b. If a radial crack exists at the hole ($\bar{r} = 1$), and if the crack propagation depends on only the magnitude

of $\bar{\sigma}_\theta$, then a step compression input ($\bar{\sigma}_r = -1$) is more critical than a static $\bar{\sigma}_r$ load; and a rectangular input, with a width of $\tau = 3.88$ is more severe than the step input. Fig. 6d is a schematic sketch illustrating this point.

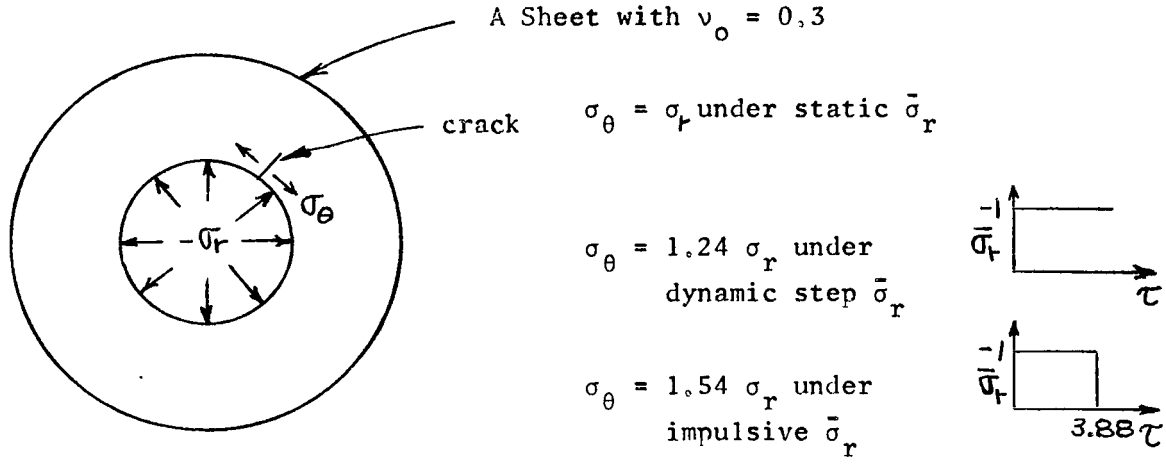

Figure 6d Rectangular (Impulsive) σ_r Input

Under certain circumstances, a dynamic stress is not critical in initiating crack propagation because of its short duration of action. Under these circumstances a repeated rectangular load with a period of 2 x 3.88, will be most critical for crack propagation. The critical pressure ($-\sigma_r$) will be 65 percent (1/1.54 = .65) of the static pressure that would be required to initiate the crack propagation.

D. A Step $\bar{v}$ Input in Sheets

This is the second problem treated by Kromm [4], using the Laplace transform method. Our results are presented in Fig. 7 in

the form of curves of $\bar{\sigma}_r$, $\bar{\sigma}_\theta$, and $\bar{v}$ plotted against τ, with $\bar{r}$ as a parameter. Again, our results show complete agreement with Kromm's, and the curves from the two methods coincide. Many interesting features of the solution of this problem have already been discussed by Kromm. These include the asymptotic behavior of the stresses; the particular radius ($\bar{r} = 1.533$) at which $\bar{\sigma}_r$ immediately behind the wave front remains stationary; for $\bar{r} < 1.533$, $\bar{\sigma}_r$ increases monotonically, and for $\bar{r} > 1.533$, $\bar{\sigma}_r$ first decreases and then increases.

E. Step $\bar{\sigma}_r$ Input in Hollow Spheres

Fig. 8 gives the result of a unit step $\bar{\sigma}_r$ input applied at the hole ($\bar{r} = 1$) inside a sphere ($N = 2$, $\nu_o = 0.3$). The general behavior of the stresses and particle velocity is the same as that of the sheet. The oscillation of $\bar{\sigma}_r$, $\bar{\sigma}_\theta$, and $\bar{v}$ at different $\bar{r}$ is more pronounced than that for the sheet. The time required for the stresses to reach their static values is a little longer. The initial positive value of $\bar{\sigma}_\theta$ is $0.429 = \nu_o/(1 - \nu_o)$, in agreement with eq. (26). Notice that this is much higher than 0.3, the value for the sheet. Subsequently, the value of $\bar{\sigma}_\theta$ surges to a value of -0.75 at $\tau = 2.26$, and then approaches the static value of -0.5. The peak $\bar{\sigma}_\theta$ due to step $\bar{\sigma}_r$ input is, therefore, 50 percent above the static value. This is also higher than the corresponding value of 24 percent in the case of sheets. The time when the peak $\bar{\sigma}_\theta$ occurs, $\tau = 2.26$ (or $t = 2.5$ sec. for $r_o = 0.25$ in. and $E_o = 30 \times 10^6$ psi), is considerably sooner than $\tau = 3.88$, the corresponding value for sheets.

F. Ramp $\bar{\sigma}_r$ Input in Hollow Spheres

The results of this case are shown in Fig. 9. Comparing these results with those shown in Fig. 8 due to a step $\bar{\sigma}_r$ input, it can be seen that the peak stresses (except $\bar{\sigma}_r$ at $\bar{r} = 1$) and peak velocities at different $\bar{r}$ are smaller. The stresses and velocities have less oscillation. In all curves, there are no sharp wave fronts. The curves for $\bar{\sigma}_r$ and $\bar{v}$ are continuous but have discontinuities in their derivatives with respect to time. These discontinuities are propagated from the original input at $\bar{r} = 1$, $\tau = \bar{k}$, with a velocity c_2.

G. A Rectangular $\bar{\sigma}_r$ Input in Hollow Spheres

This is the impulsive input similar to the one discussed above for sheets. As shown in Fig. 10b, the absolute value of the peak $\bar{\sigma}_\theta$ is 1.18, which is 136% higher than the static value of 0.5. Thus this case is even more severe than the impulsive loading in sheets.

H. $\bar{v}$ Inputs in Hollow Spheres

Calculations have been made for a step $\bar{v}$ input and a ramp $\bar{v}$ input, but the results are not presented here. The general discussions for the corresponding cases in sheets are all applicable to these spherical cases. The ramp $\bar{v}$ inputs with decreasing values of $\bar{k}$ approach the step $\bar{v}$ input.

I. Exponential σ_r Input in Hollow Spheres

The input in this case is an exponential function, $\sigma_r = p_o e^{-\alpha t}$, applied at the hole. Extensive calculations have been performed for this problem by Allen and Goldsmith [10] with an electronic calculator, using the Laplace transform solution by Sharpe [9] as a basis. This input has special significance in simulating the effect of explosive

charge detonated in contact with a metal. It also has practical applications in underground explosions and in geophysics. The purpose of the inclusion of this case is to demonstrate the accuracy and ease of application of the present method. The same dimensional constants for steel are used in the present method as in [10]. These are:

E_o = 2.139 megabars $\quad$ p_o = 0.283 megabars

ρ = 7.849 g/cc $\quad$ α = 2 sec^{-1}

ν_o = 0.31 $\quad$ r_o = 1.5 cm

The results are shown in Fig. 11, in the form of σ_r, σ_θ, and v vs. r curves, with t as a parameter. The results from [10] are indistinguishable from these curves by the present method, except the σ_r curve with t = 2μsec in Fig. 11a. Here, our results show a dip while Ref. [10] gives no dip. It is believed that our results are correct and a slight error in involved in [10].

VI. CONCLUSIONS

A. The method of characteristics has been successfully applied to the propagation of cylindrical and spherical dilatational waves in elastic media. Its simple recurrent finite-difference equations are most adaptable to computer calculations. It can readily give numerical solutions to problems with any input functions.

B. Step inputs, in both σ_r and v, produce more severe stress conditions than corresponding ramp inputs. Ramp inputs, with decreasing rising time, approach the step input as a limit. Thus, the step input should be used in calculating the upper bounds of dynamic stresses.

C. For the case of a step σ_r input applied to a sheet, the maximum σ_θ is 24 percent higher than the static value. For a rectangular pulse input with proper width, the σ_θ could be 54 percent higher than the static value. The corresponding numbers for the hollow sphere are 50 percnet for step σ_r and 136% for rectangular impulse input. These transient peak stresses may be of significant importance in the dynamic crack propagation and the dynamic strength of materials.

D. The method of characteristics could be easily extended to other elastic wave problems, such as, the bending of plates including shear effect and rotary inertia, non-linear large deflection equations, and possibly even to bodies with two space variables.

VII. REFERENCES

1. Leonard, R. W., and Budiansky, B., "On Traveling Waves in Beams," NACA TN 2874, 1953.

2. Jahsman, W. E., "Propagation of Abrupt Circular Wave Fronts in Elastic Sheets and Plates," Proc. of the 3rd Nat. Congress of Appl. Mech., 1958, pp. 115-202.

3. Kromm, A., "Zur Ausbreitung von Stoßwellen in Kreishochscheiben," Z. angew. Math. Mech. Bd. 28, Nr. 4, April 1948, pp. 104-114.

4. Kromm, A., "Zur Ausbreitung der Stoßwellen in Kreislochscheiben," Z. angew. Math. Mech. Bd. 28, Nr. 10, Okt. 1948, pp. 297-303.

5. Miklowitz, J., "Plane-Stress Unloading Waves Emanating From A Suddenly Punched Hole in a Stretched Elastic Plate," Jour. of Appl. Mech., March 1960, pp. 165-171.

6. Selberg, H. L., "Transient Compression Waves from Spherical and Cylindrical Cavities," Arkiv för Fysik, Vol. 5, 1952, pp. 97-108.

7. Kolsky, H., "Stress Waves in Solids," Dover Publications, Inc. New York, 1963.

8. Hopkins, H. G., "Dynamic Expansion of Spherical Cavities in Metals," Progress in Solid Mechanics, Vol. I, North-Holland Publishing Co., Amsterdam, 1960.

9. Sharpe, H. A., "The Production of Elastic Waves by Explosion Pressures. I. Theory and Empirical Field Observations," Geophysics Mag., Vol. 7, 1942.

10. Allen, W., and Goldsmith, W., "Elastic Description of a High-Amplitude Spherical Pulse in Steel," Jour. of Appl. Phys., Vol. 26, No. 1, January 1955.

11. Kinslow, R., "Properties of Spherical Stress Waves Produced by Hypervelocity Impact," Arnold Engineering Dev. Center Report No. AEDC-TDR-63-197, October 1963.

12. Perzyna, P., and Bejda, J., "The Propagation of Spherical Stress Waves in a Work-hardening and Rate Sensitive Plastic Medium," Bulletin De L'academie, Polonaise Des Sciences, Serie des sciences techniques, Vol. XII, No. 4, 1964.

13. Kaliski, S., Nowacki, W. K., and Wlodarczyk, E., "Propagation and Reflection of a Spherical Wave in an Elastic-Visco-Plastic Strain-Hardening Body," Proc. of Vibration Problems, Warsaw, 1.5, 1964.

14. Courant, R., and Hilbert, D., "Methods of Mathematical Physics," Volume II, Interscience Publishers, New York, 1962.

15. Timoshenko, S., and Goodier, H. N., "Theory of Elasticity," McGraw-Hill Book Co., Inc., New York, 1951.

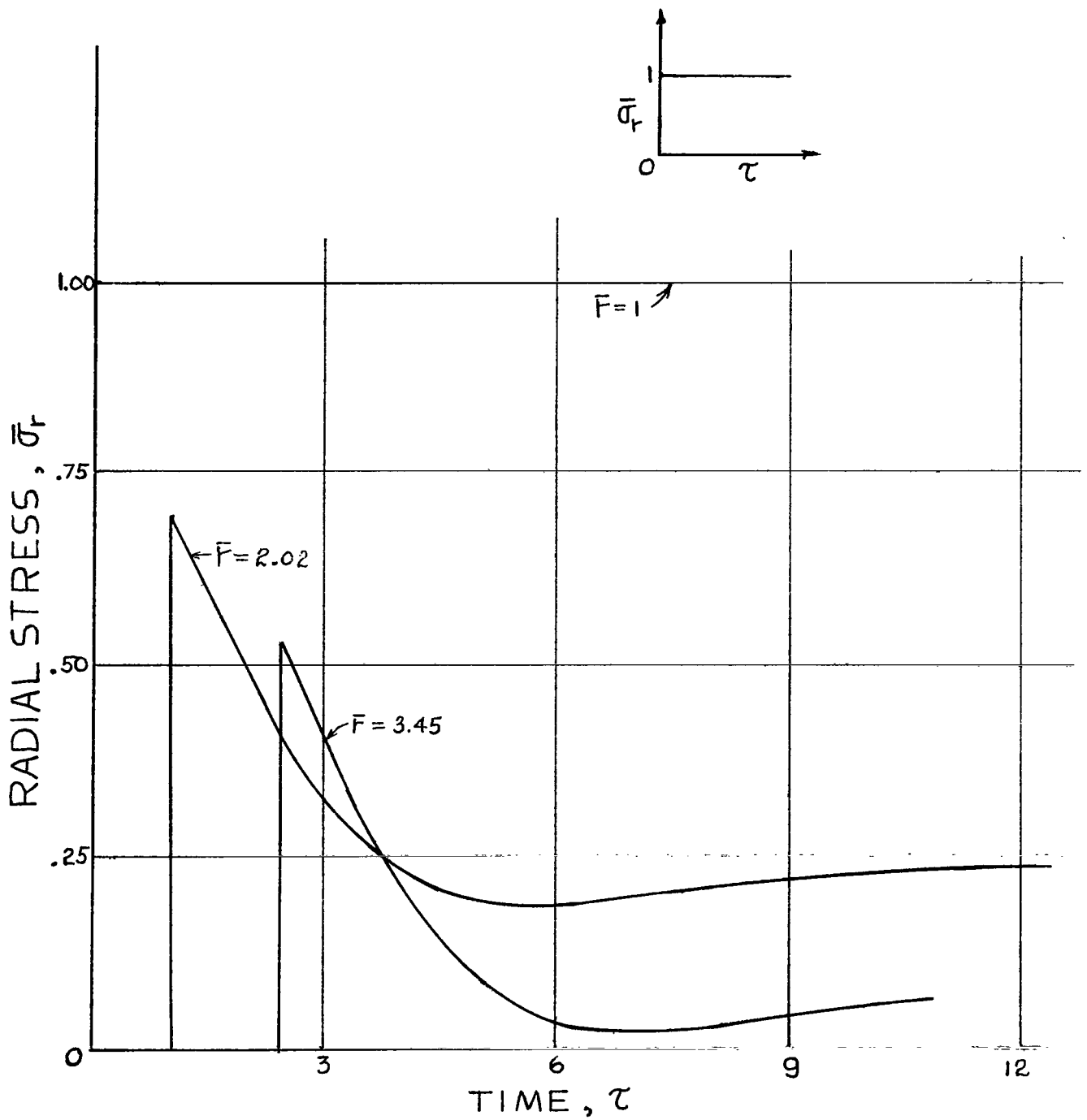

a. Radial stress, $\bar{\sigma}_r$, versus time, τ.

Figure 3 Results of Step $\bar{\sigma}_r$ Input, N = 1.

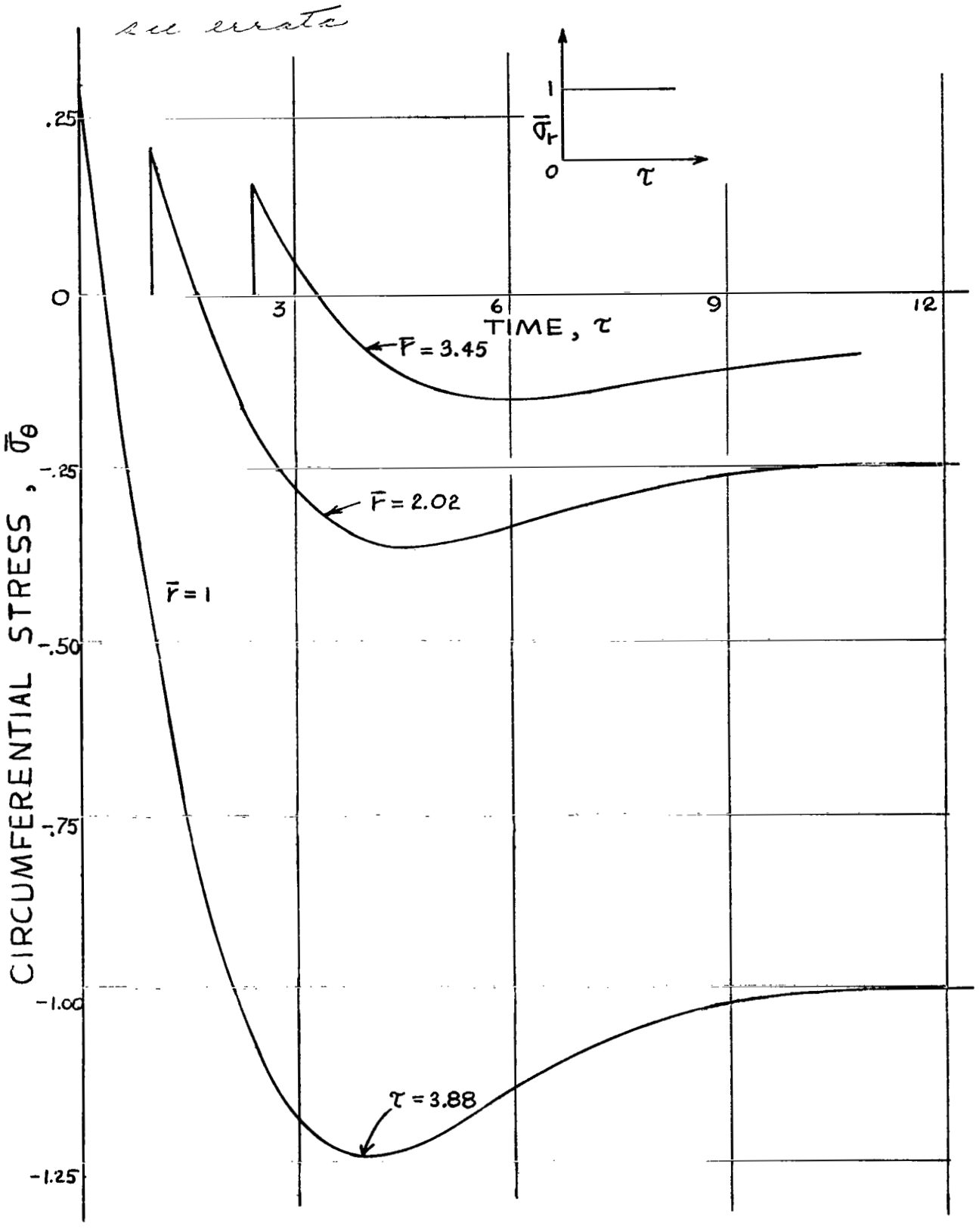

b. Circumferential stress, $\bar{\sigma}_\theta$ versus time, τ.

Figure 3 Results of Step $\bar{\sigma}_r$ Input, N = 1.

see errata

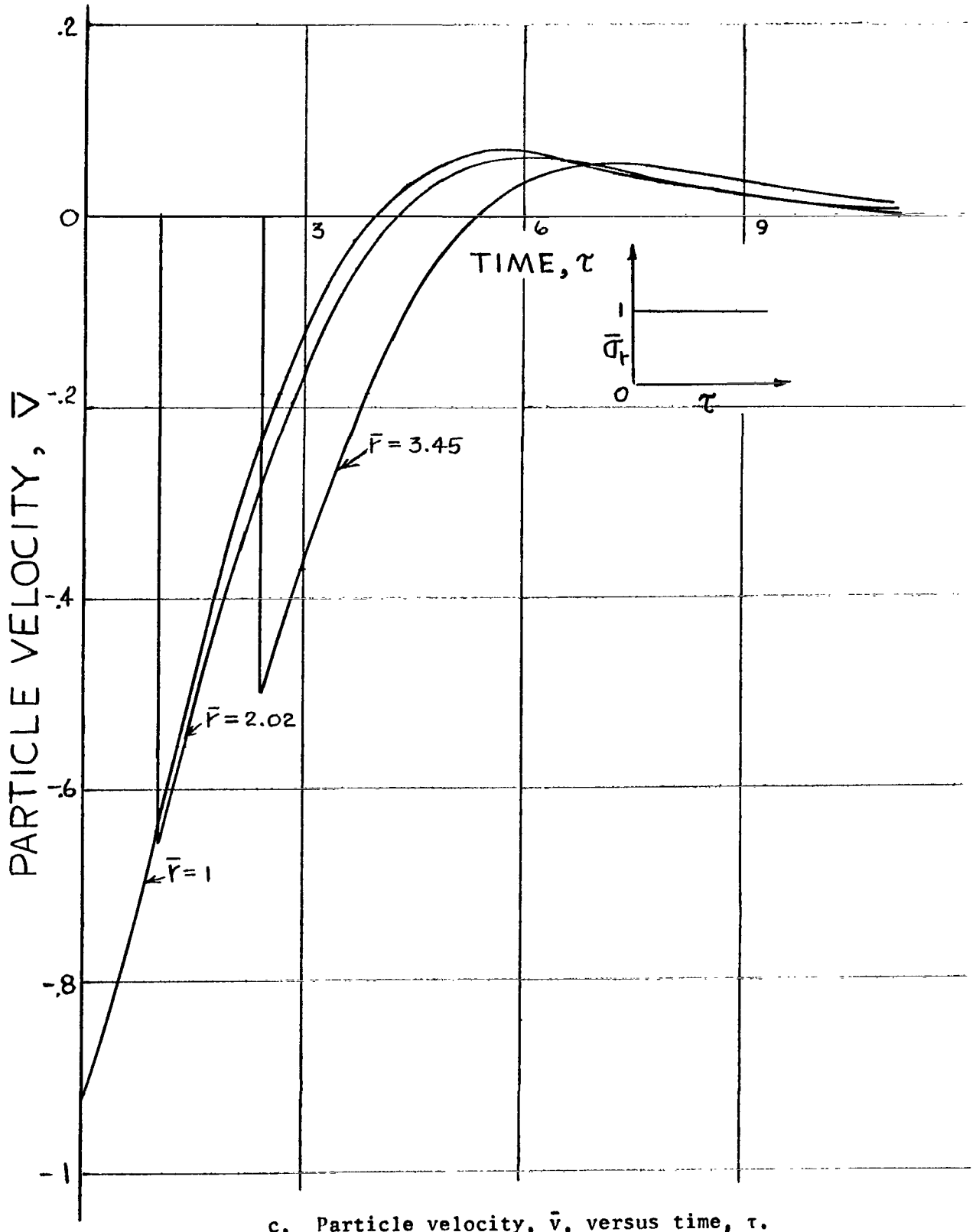

c. Particle velocity, $\bar{v}$, versus time, τ.

Figure 3 Results of Step $\bar{\sigma}_r$ Input, N = 1.

re errata

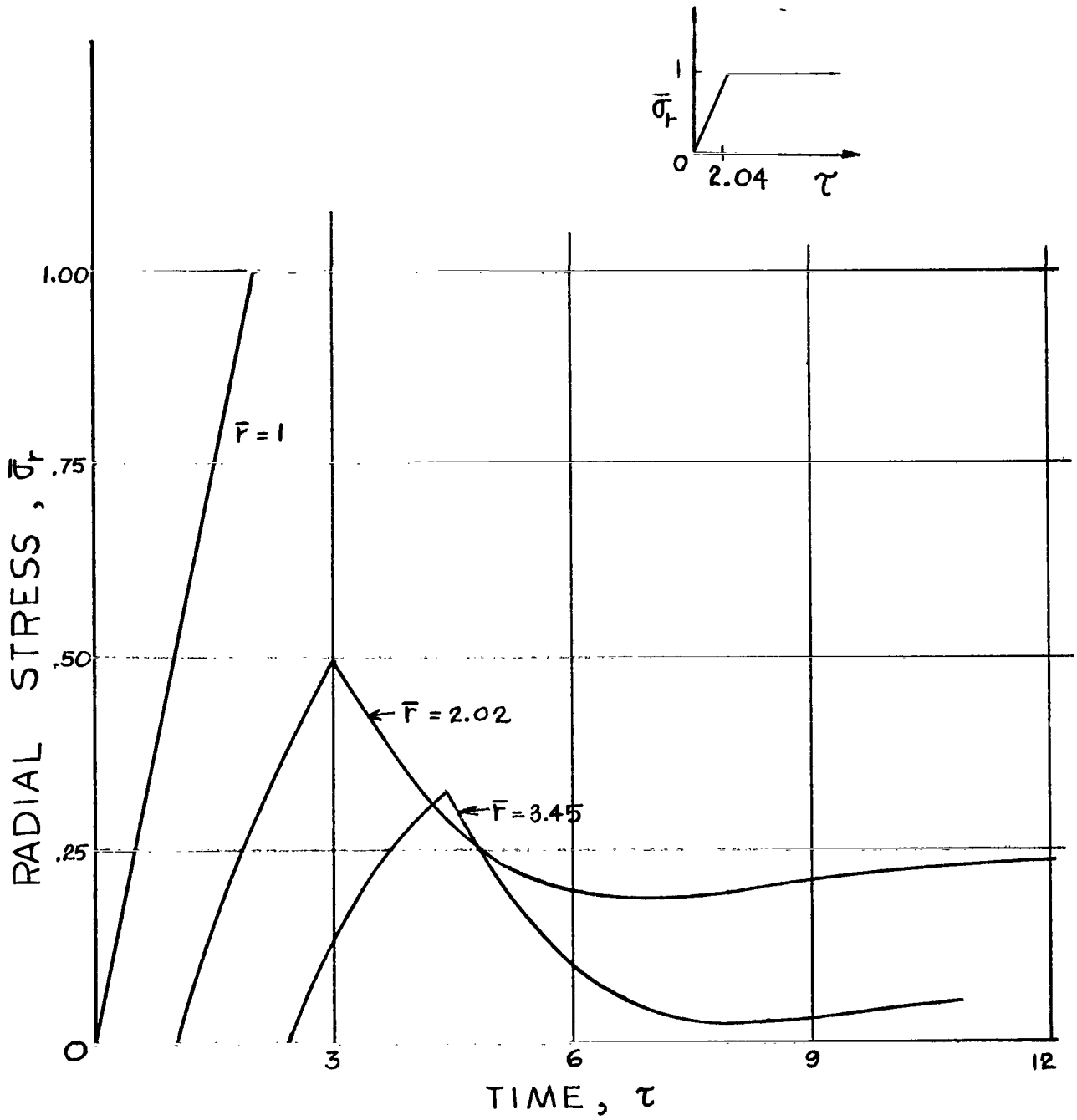

a. Radial Stress, $\bar{\sigma}_r$, versus time, τ.

Figure 4 Results of Ramp $\bar{\sigma}_r$ Input, N = 1.

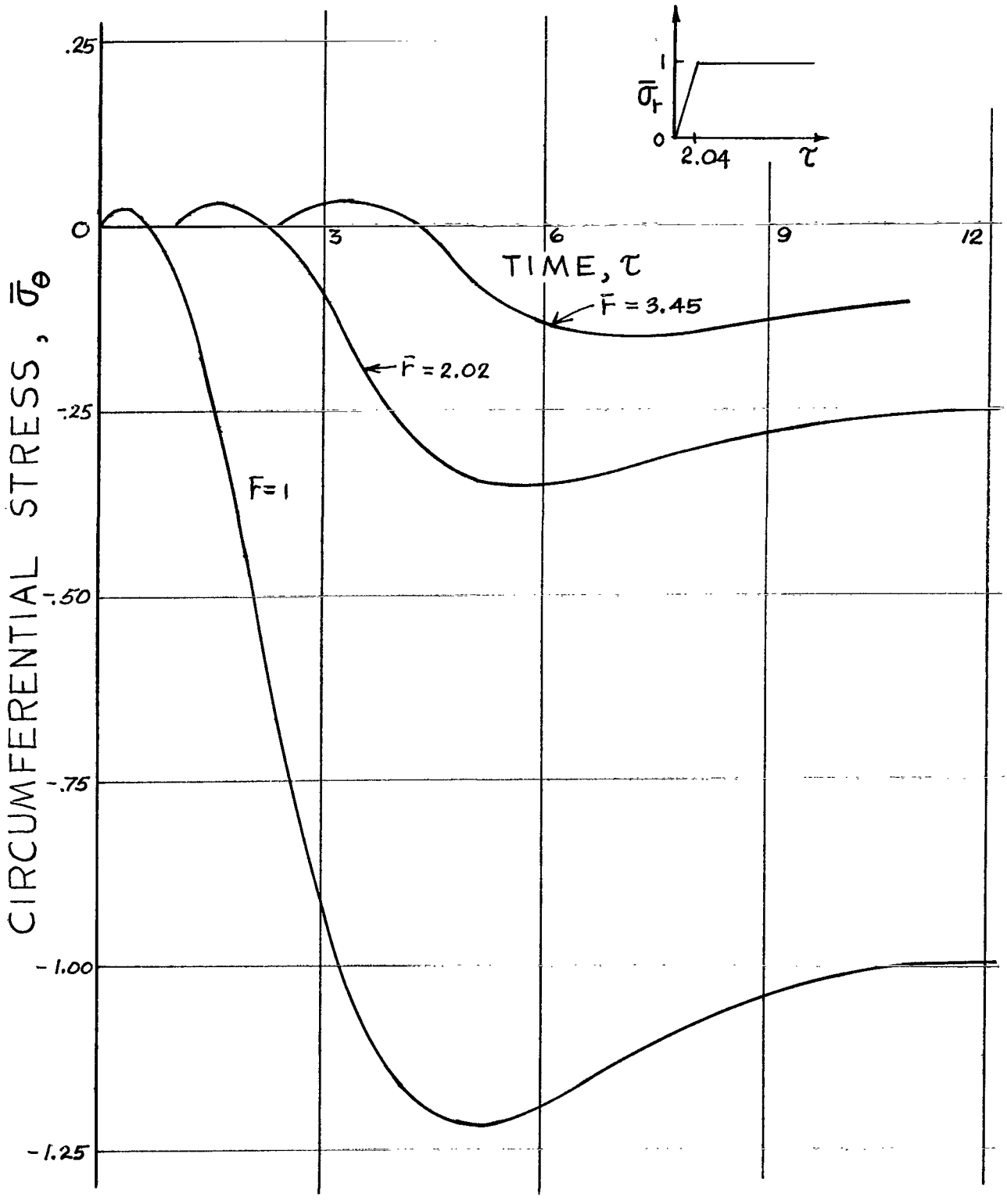

b. Circumferential stress $\bar{\sigma}_\theta$, versus time, τ.

Figure 4 Results of Ramp $\bar{\sigma}_r$ Input, N = 1.

see errata

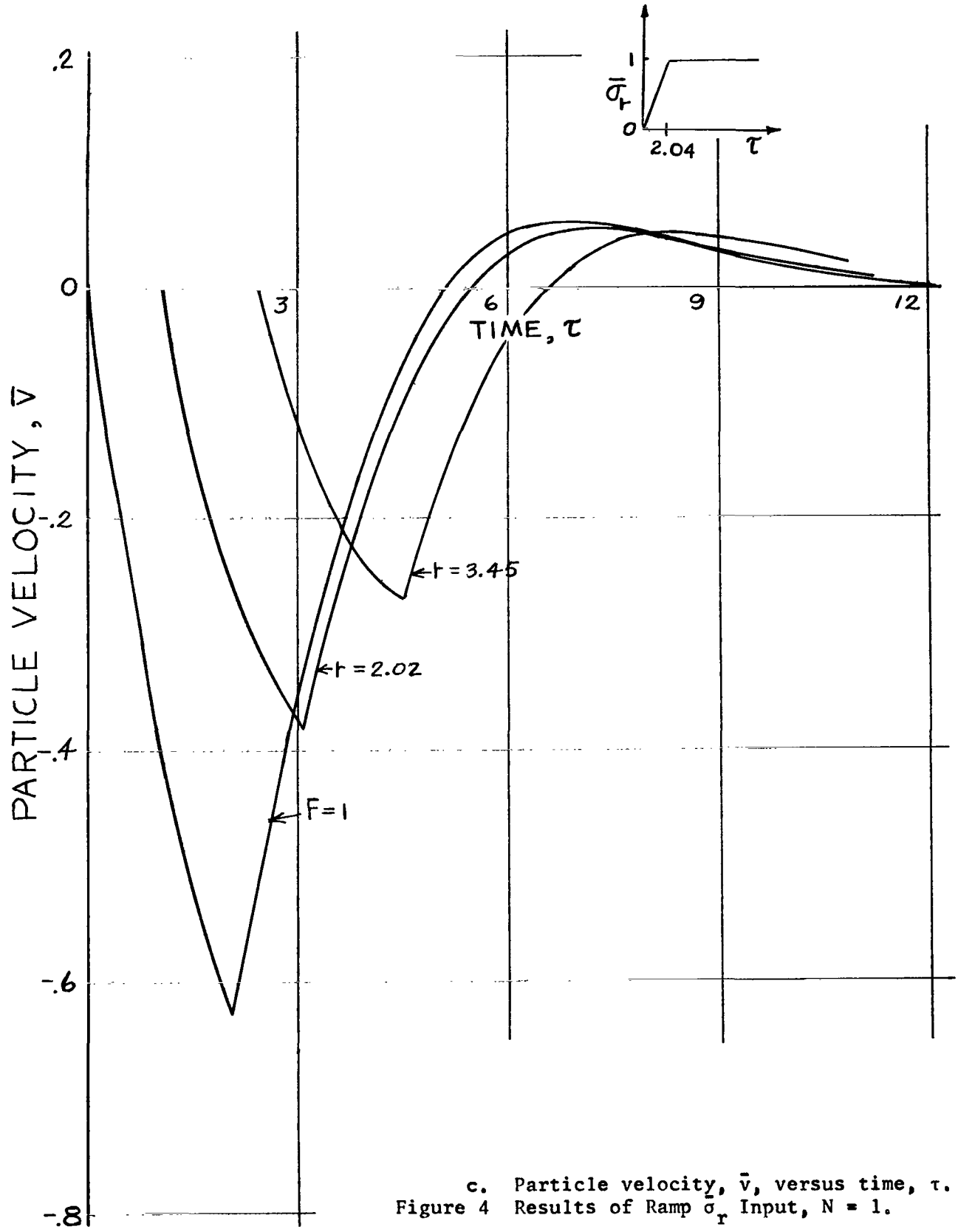

c. Particle velocity, $\bar{v}$, versus time, τ.

Figure 4 Results of Ramp $\bar{\sigma}_r$ Input, N = 1.

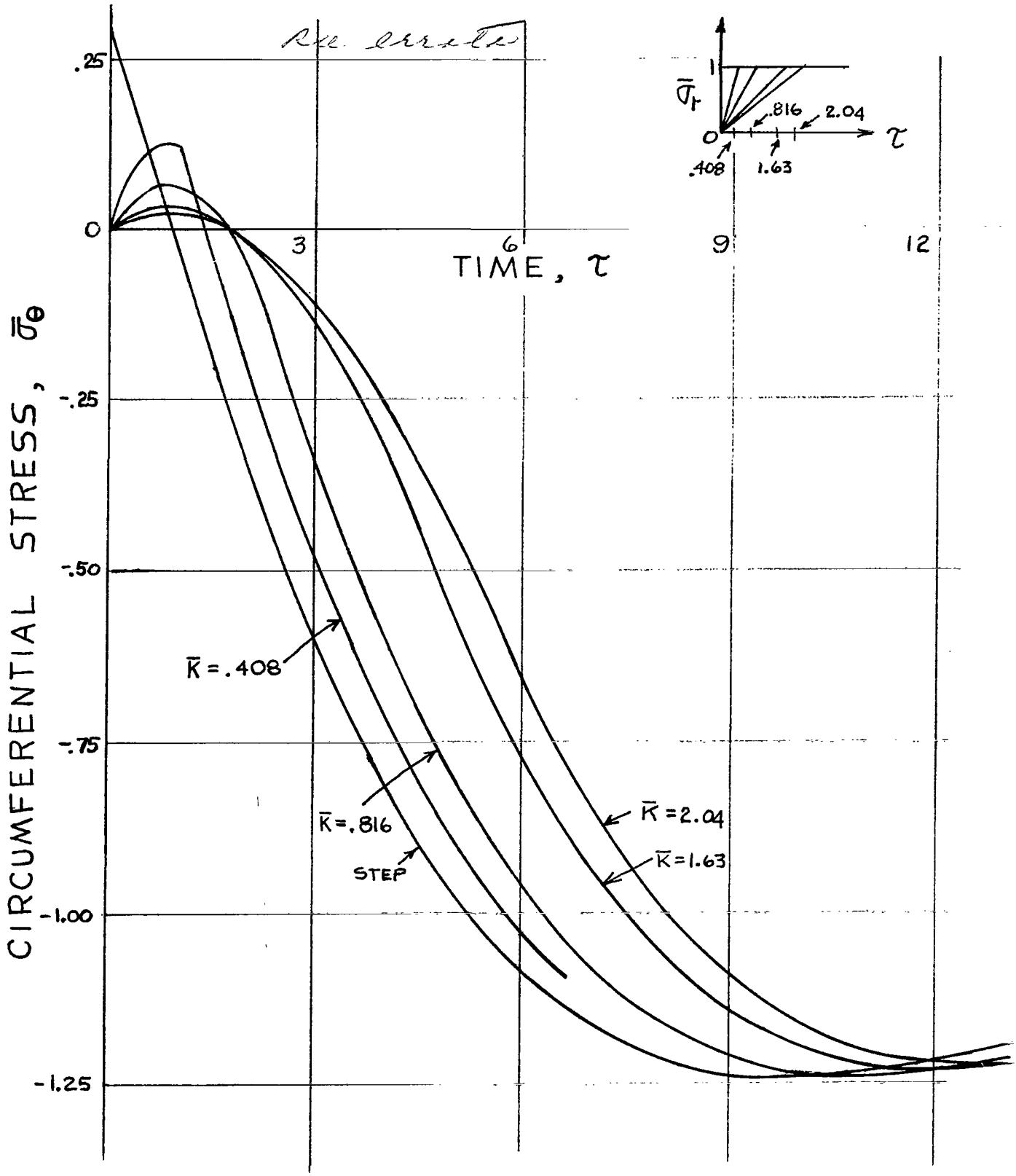

a. Circumferential stress, $\bar{\sigma}_\theta$, at $\bar{r}$ = 1, versus time, τ.

Figure 5 Results of Various Ramp $\bar{\sigma}_r$ Inputs, N = 1.

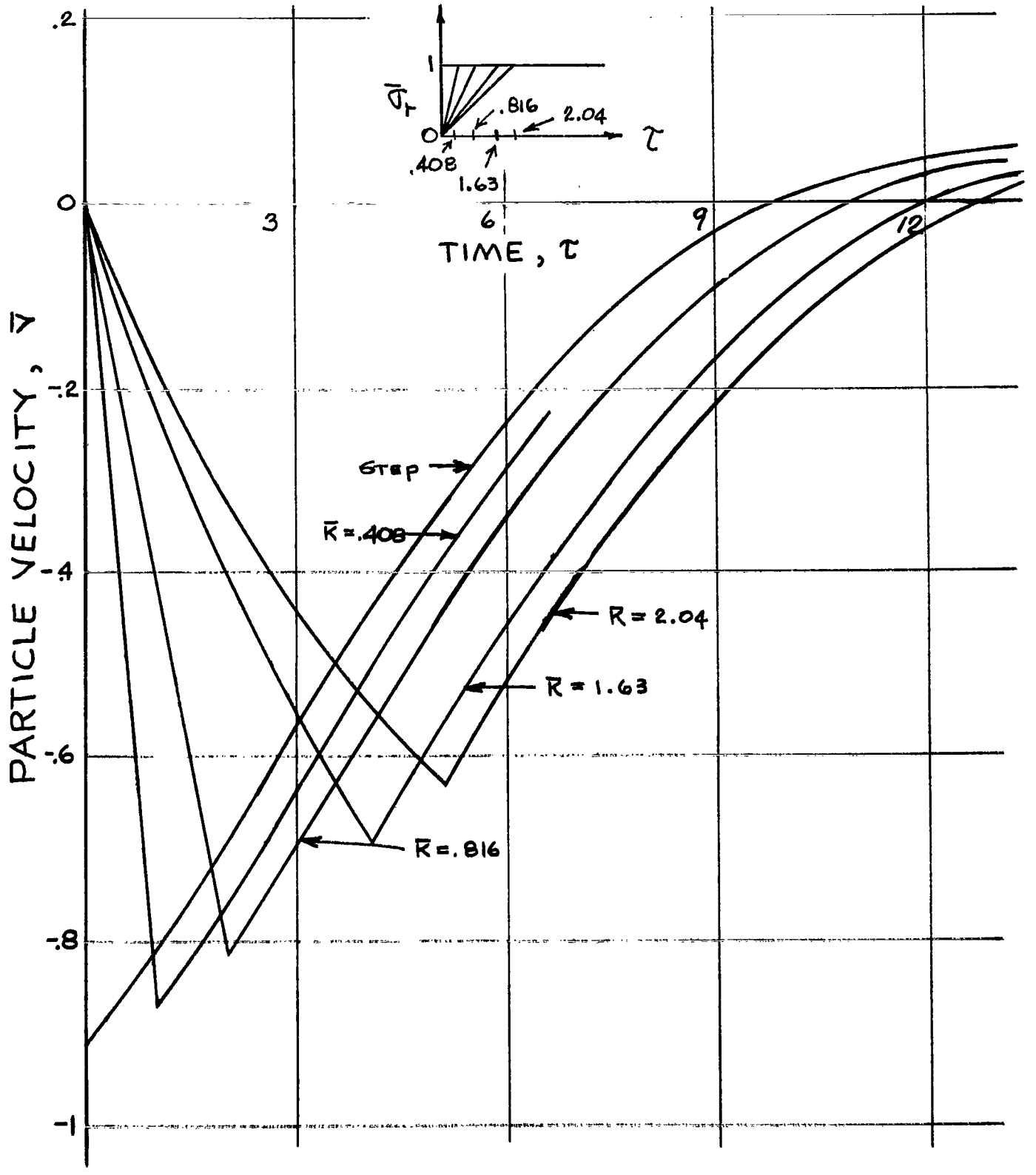

b. Particle velocity, $\bar{v}$, at $\bar{r} = 1$, versus time, τ.

Figure 5 Results of Various Ramp $\bar{\sigma}_r$ Inputs, N = 1.

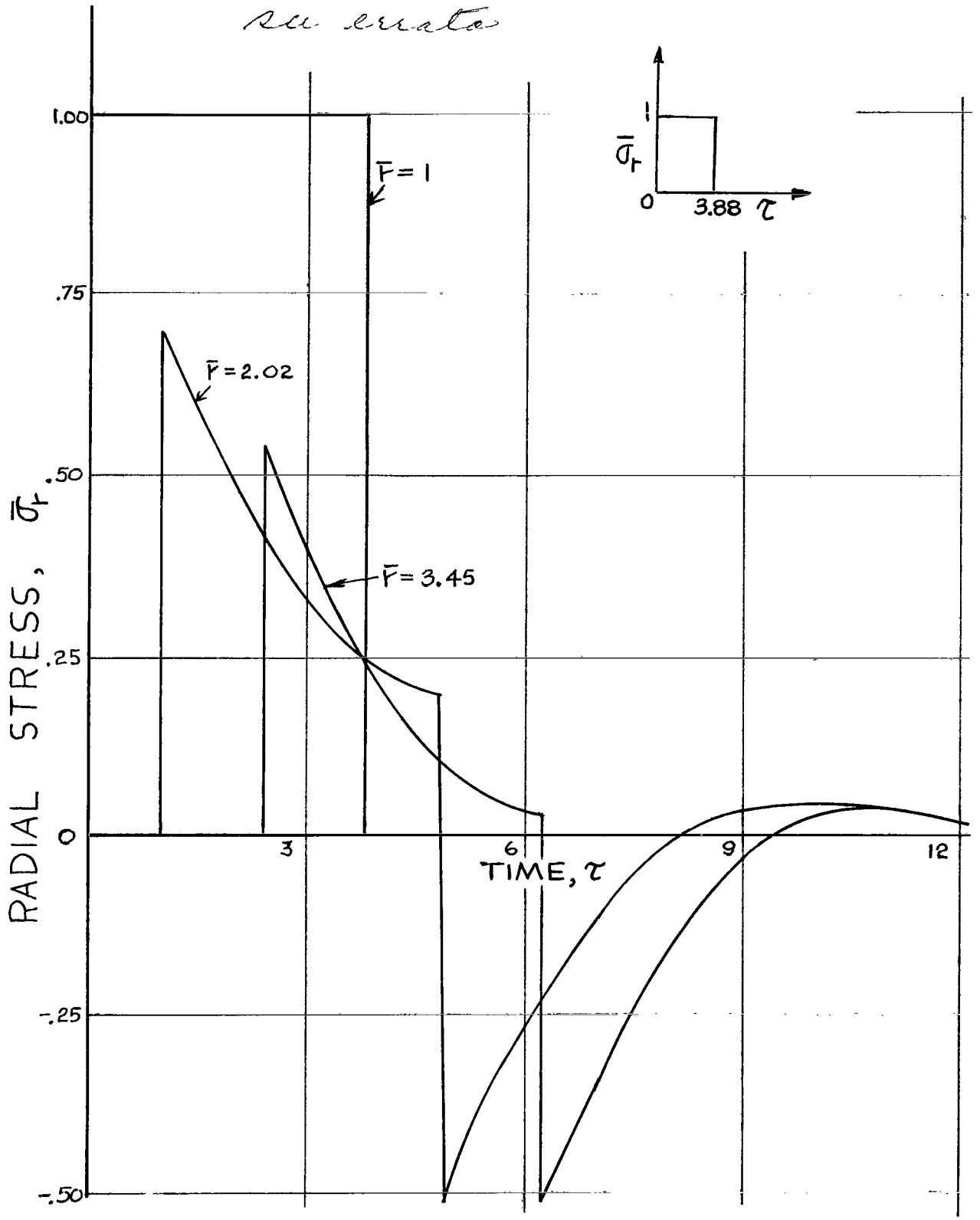

a. Radial stress, $\bar{\sigma}_r$, versus time, τ.

Figure 6 Results of Rectangular Impulse $\bar{\sigma}_r$ Input, N = 1.

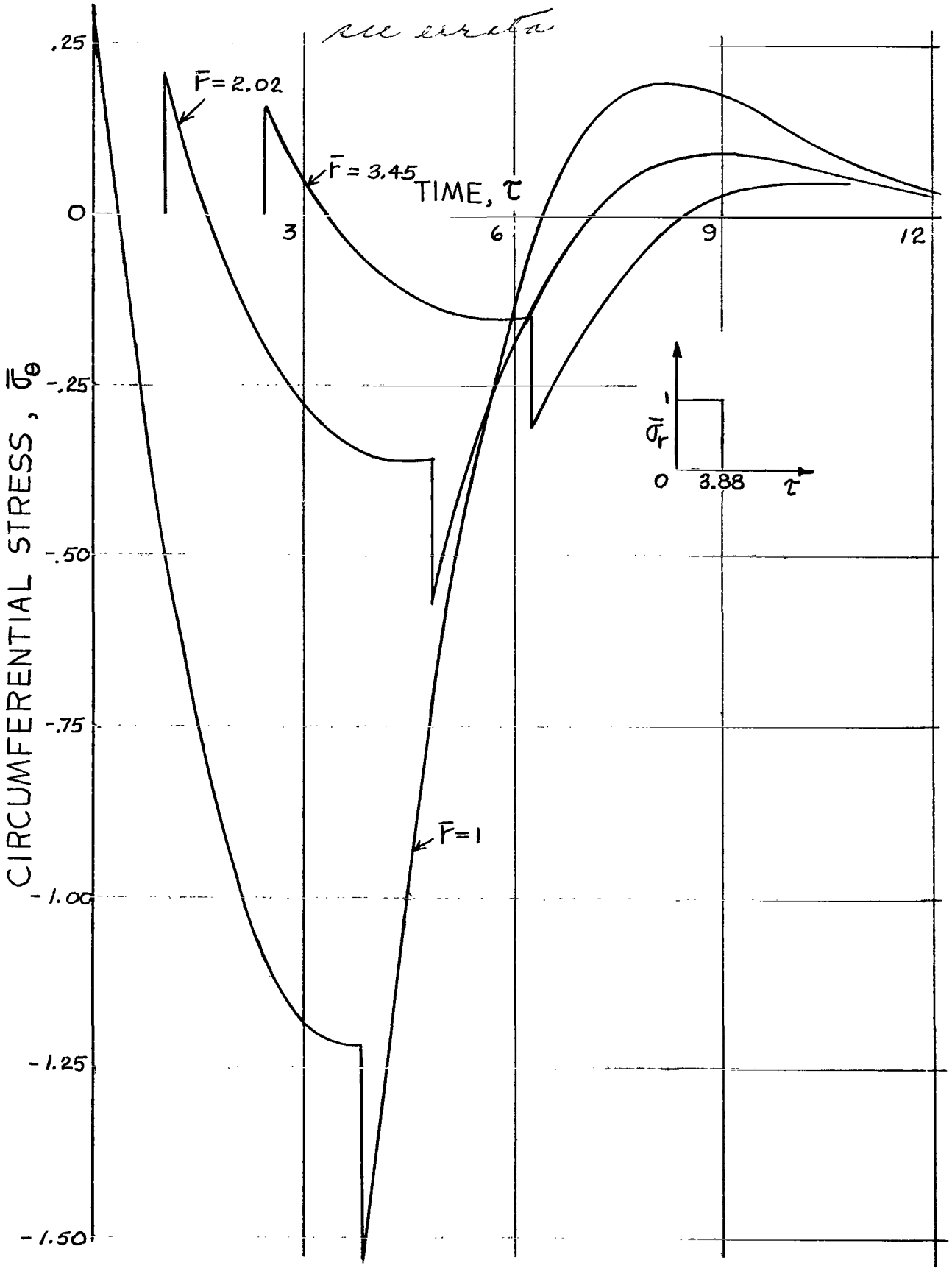

b. Circumferential stress, $\bar{\sigma}_\theta$, versus time, τ.

Figure 6 Results of Rectangular Impulse $\bar{\sigma}_r$ Input, N = 1.

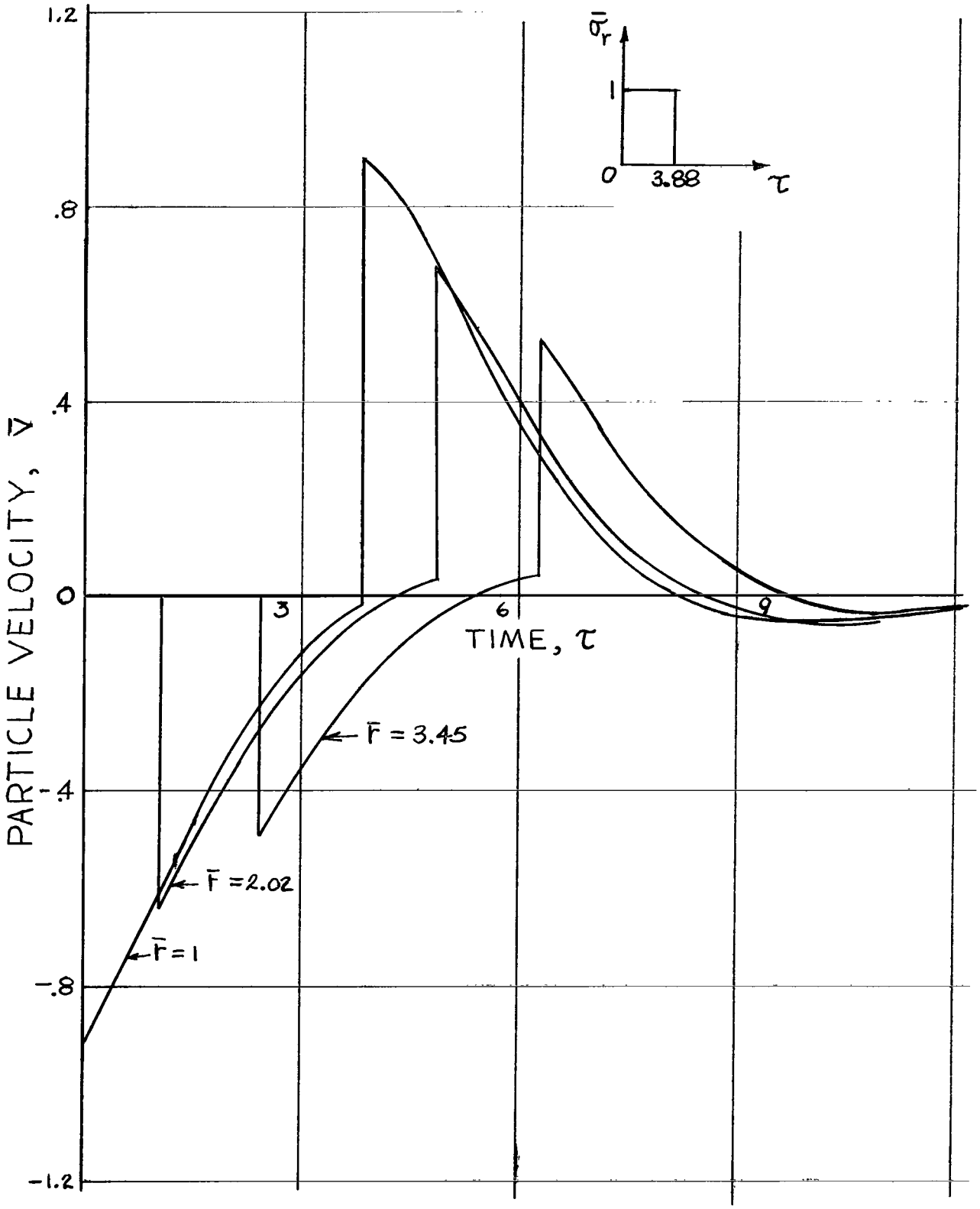

c. Particle velocity, $\bar{v}$, versus time, τ.

Figure 6 Results of Rectangular Impulse $\bar{\sigma}_r$ Input, N = 1.

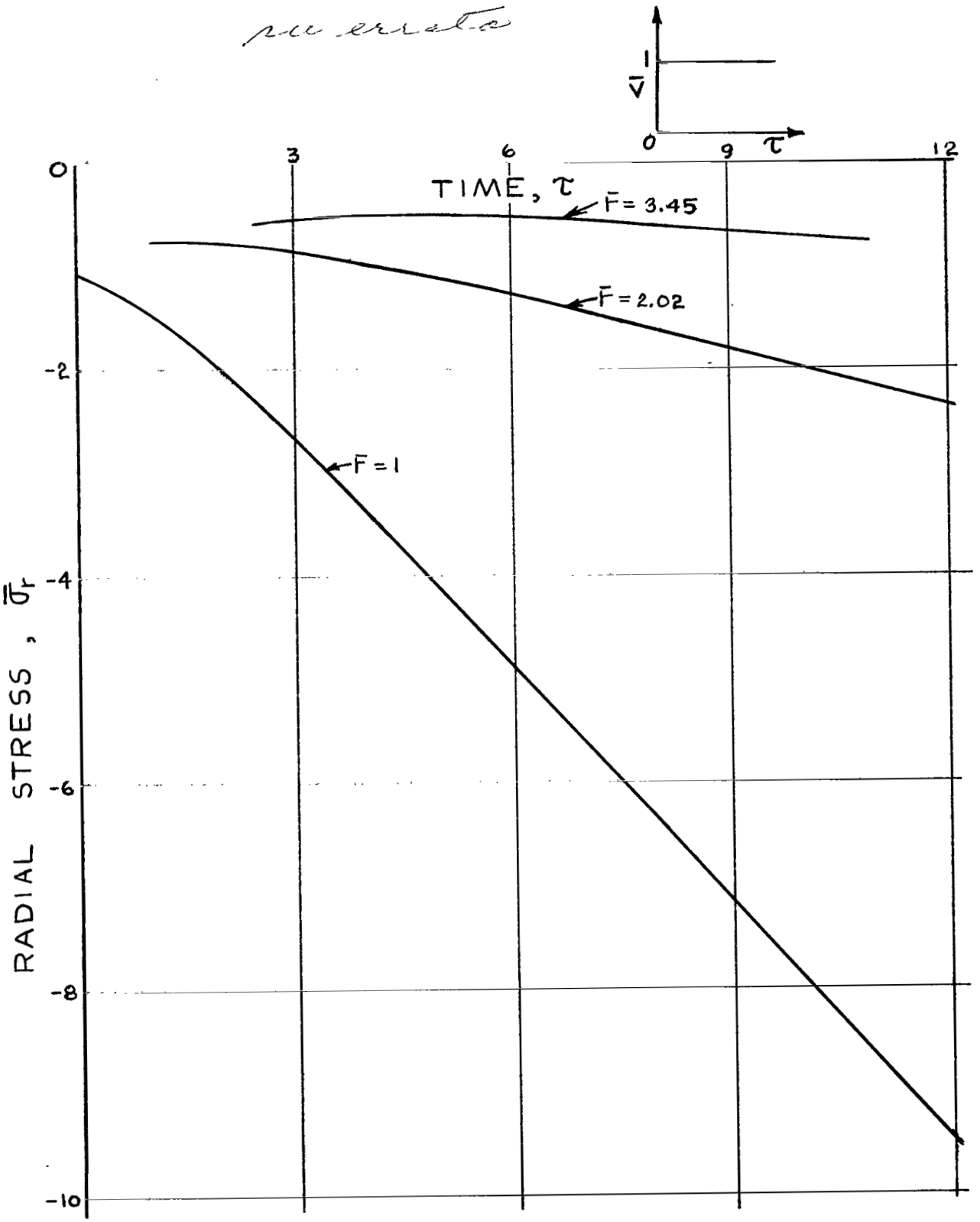

a. Radial Stress, $\bar{\sigma}_r$, versus time τ.

Figure 7 Results of Step $\bar{v}$ Input, N = 1.

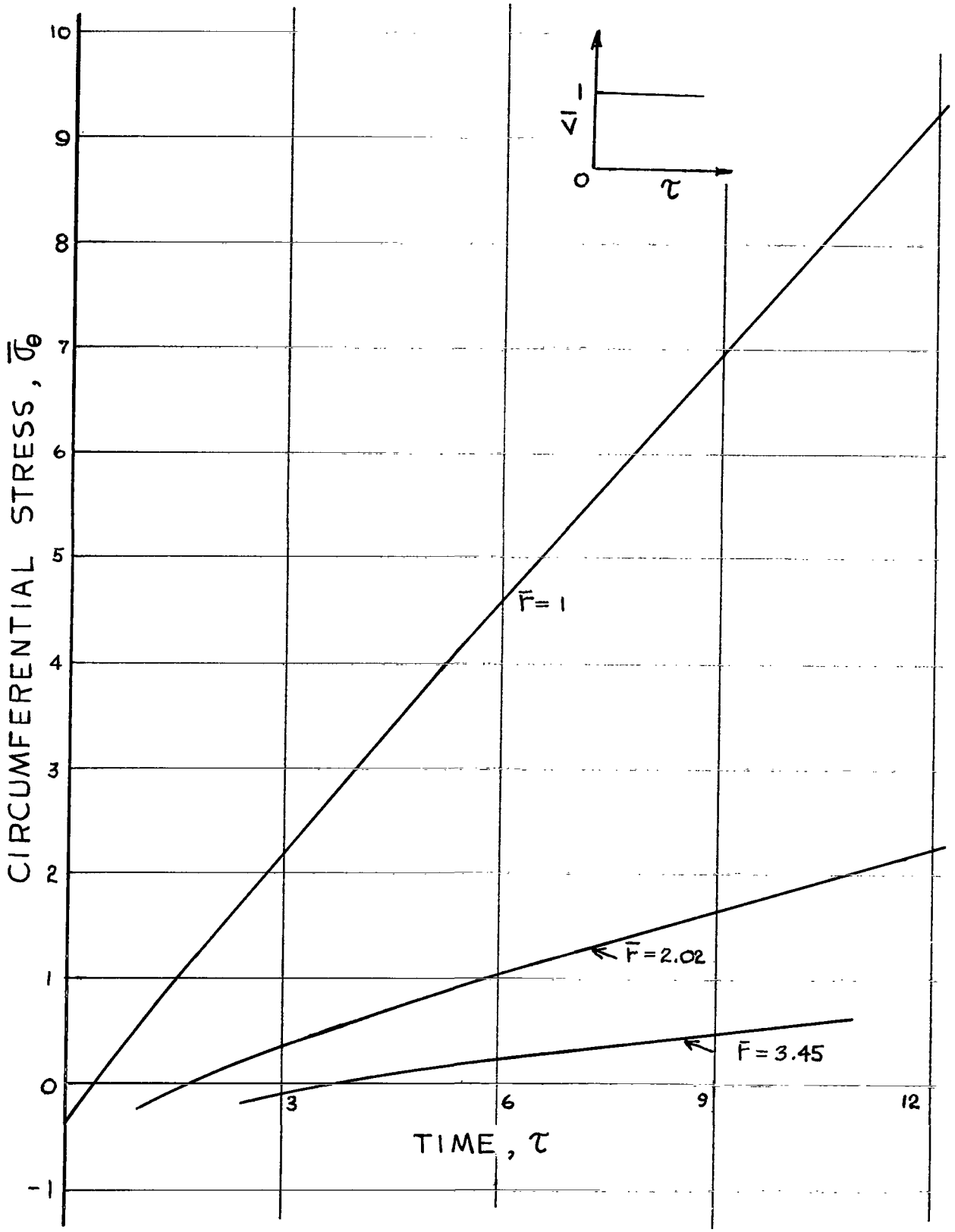

b. Circumferential stress, $\bar{\sigma}_\theta$, versus time, τ.

Figure 7 Results of Step $\bar{v}$ Input, N = 1.

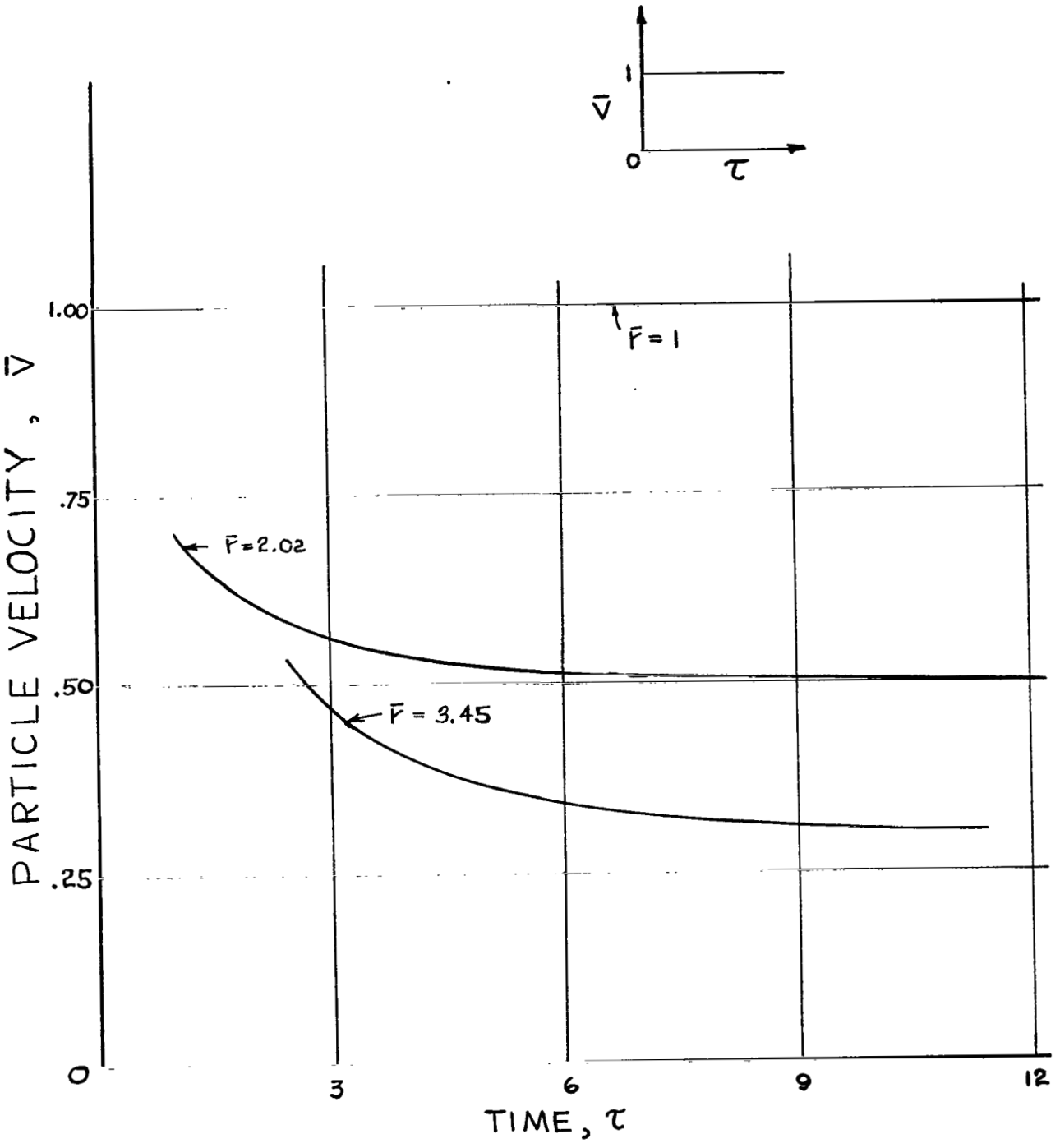

c. Particle velocity, $\bar{v}$, versus time, τ.

Figure 7 Results of Step $\bar{v}$ Input, N = 1.

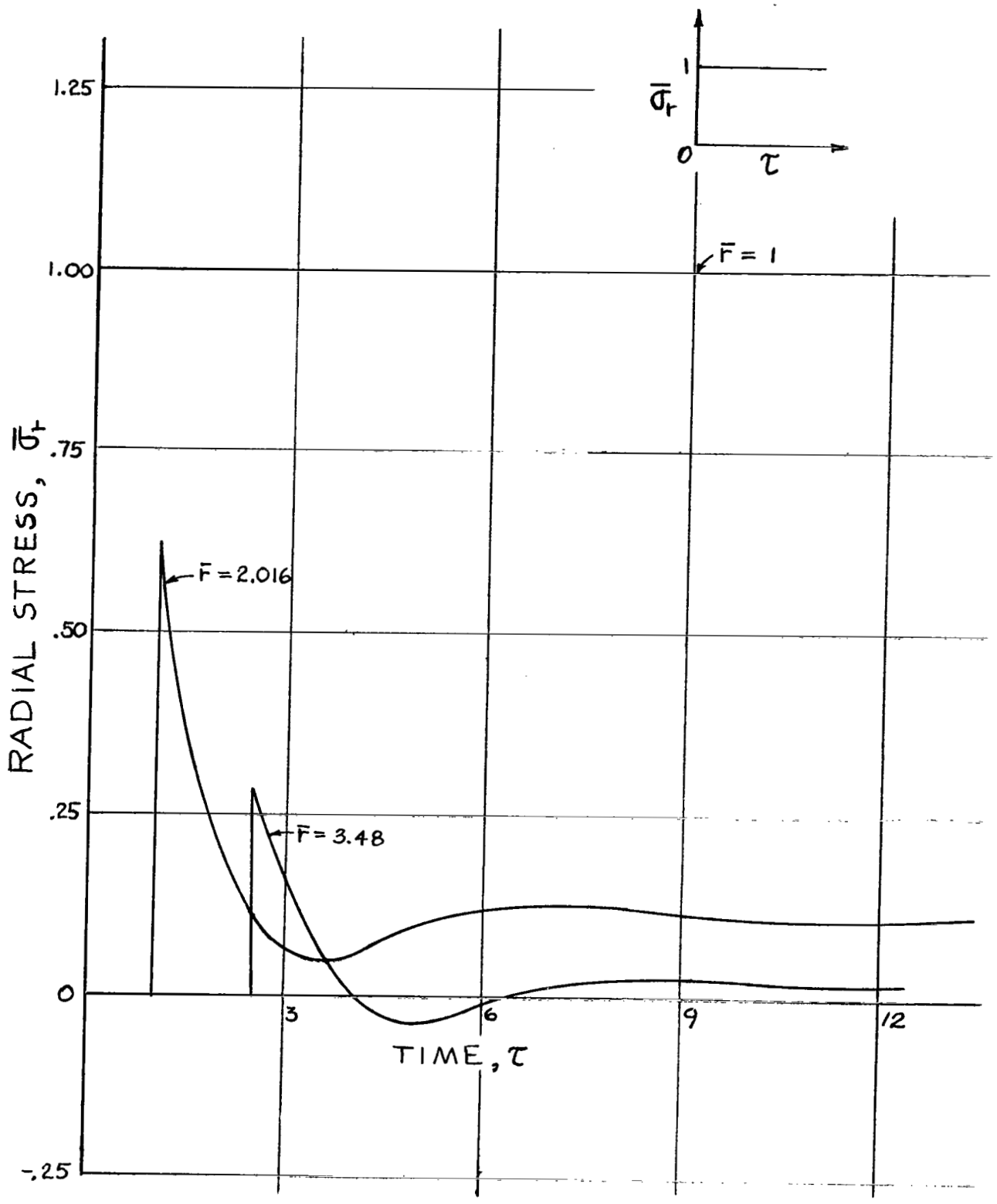

a. Radial stress, $\bar{\sigma}_r$, versus time, τ.

Figure 8 Results of Step $\bar{\sigma}_r$ Input, N = 2.

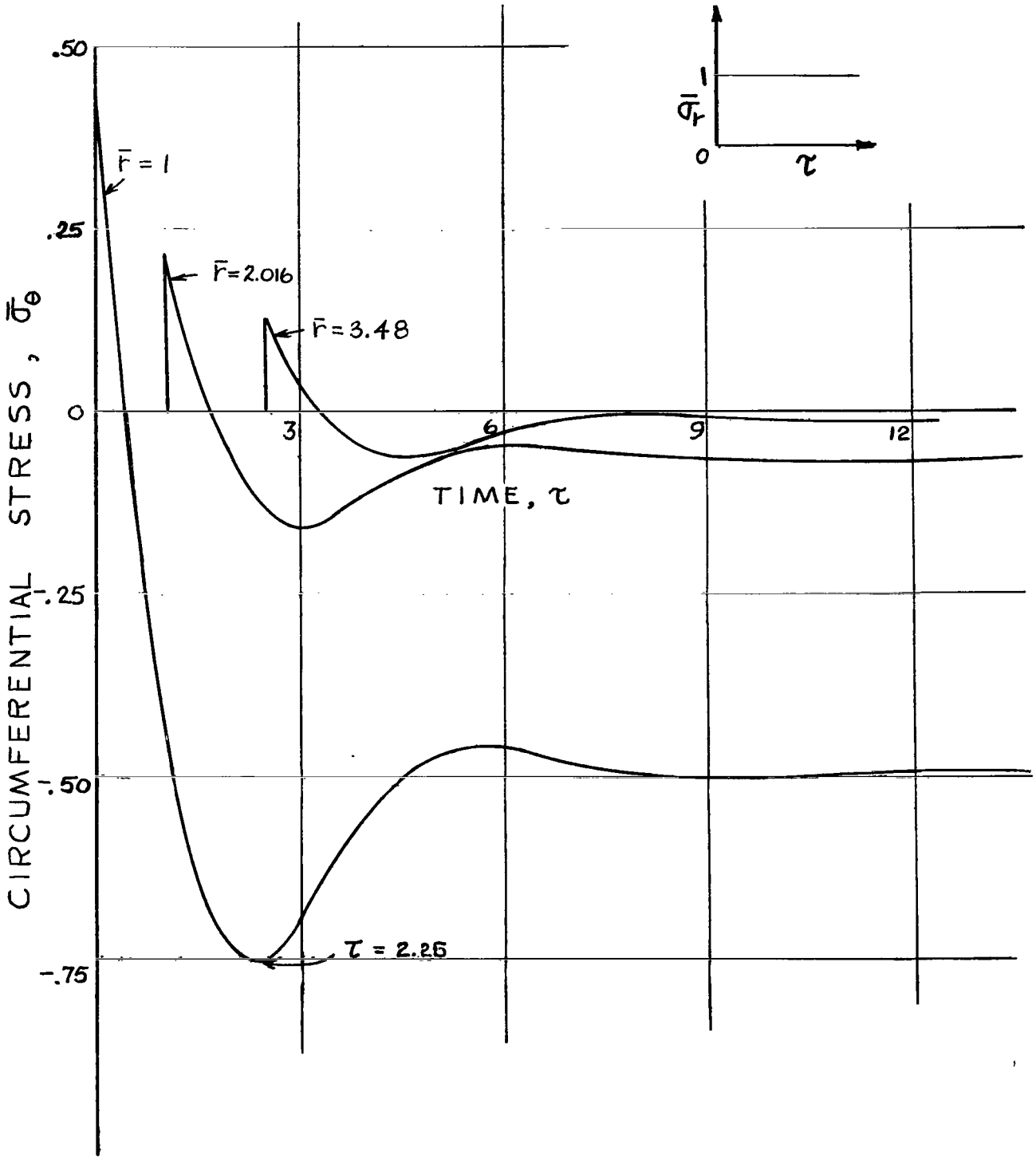

b. Circumferential stress, $\bar{\sigma}_\theta$, versus time, τ.

Figure 8 Results of Step $\bar{\sigma}_r$ Input, N = 2.

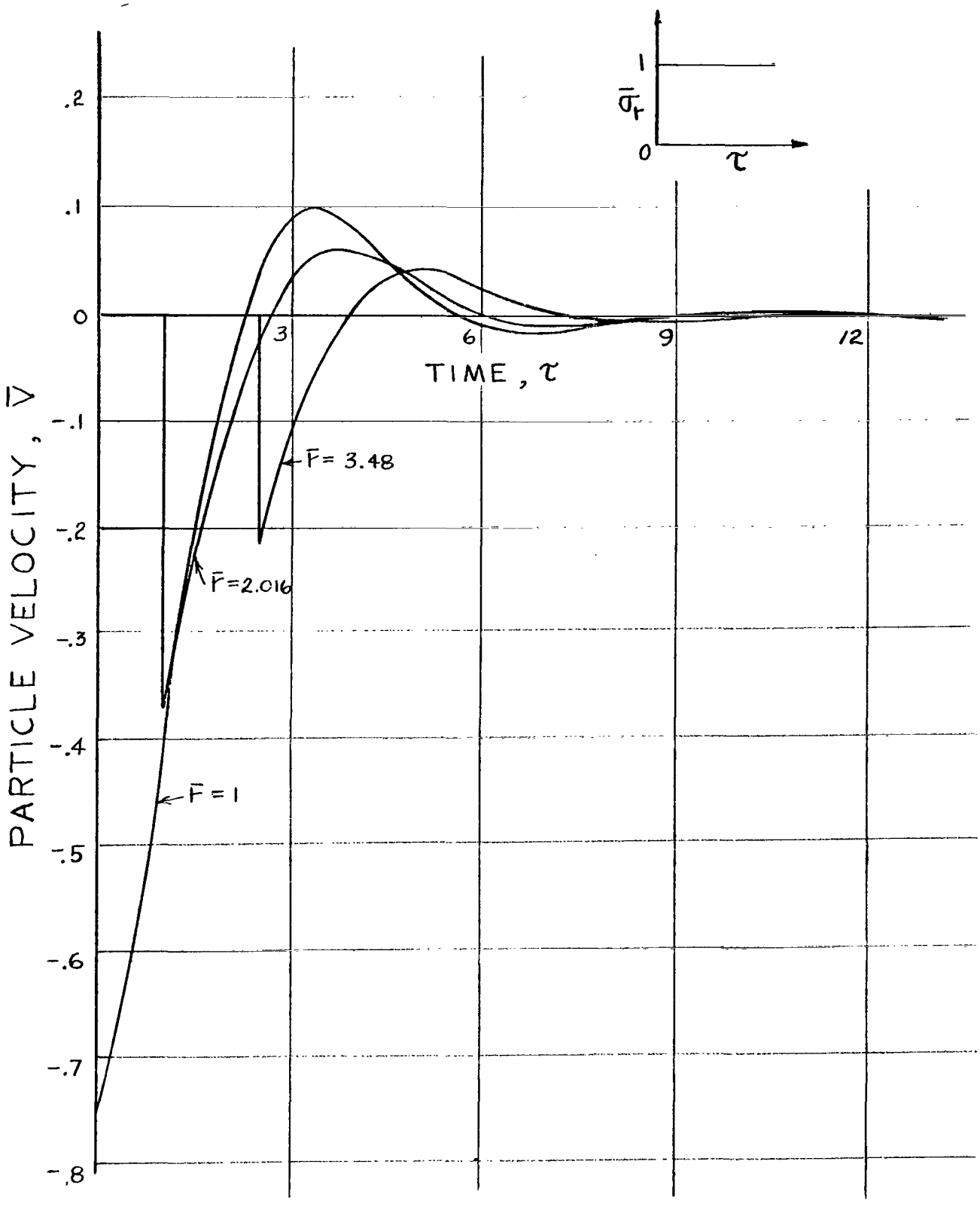

c. Particle velocity, $\bar{v}$, versus time, τ.

Figure 8 Results of Step $\bar{\sigma}_r$ Input, N = 2.

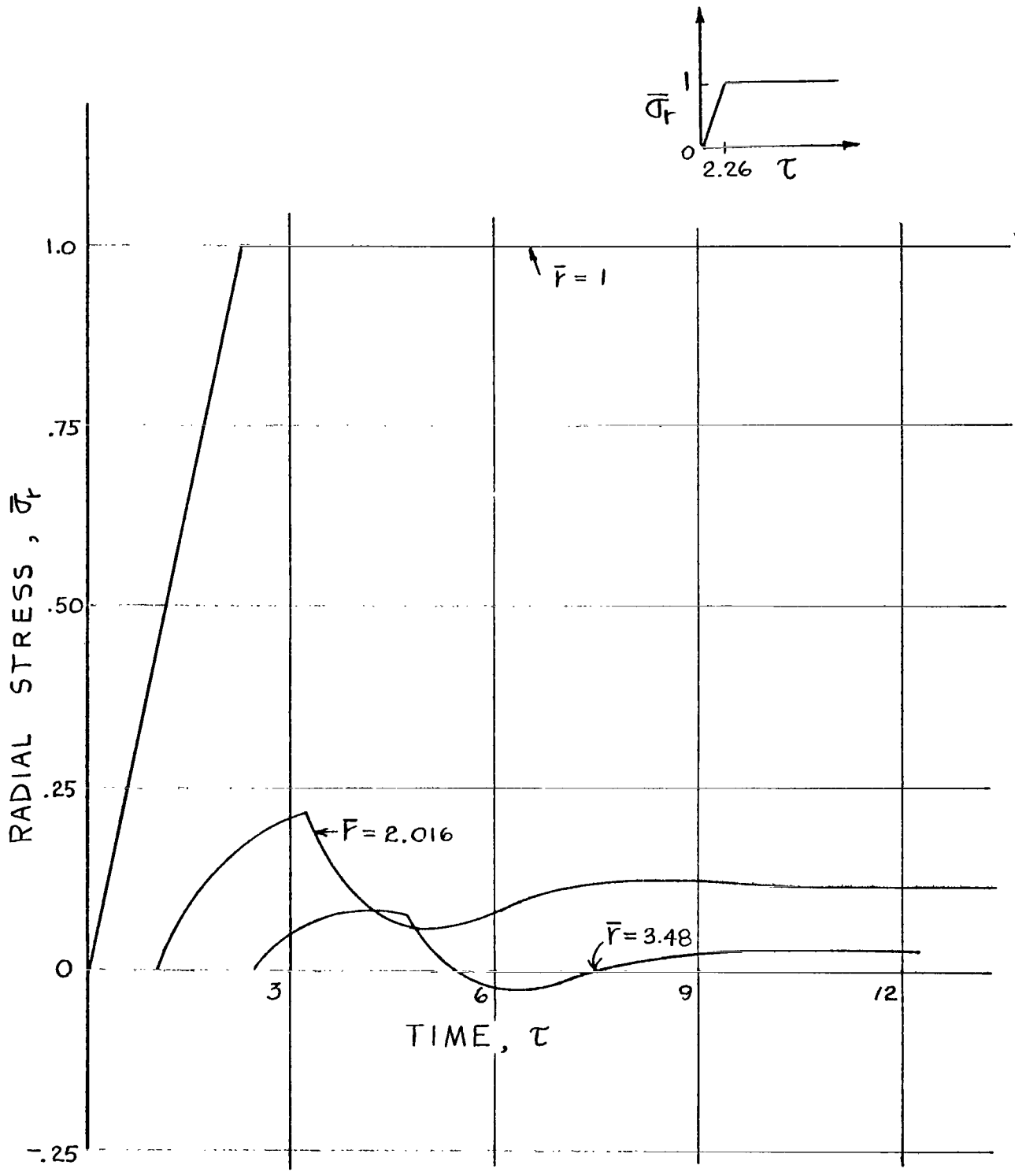

a. Radial stress, $\bar{\sigma}_r$, versus time, τ.

Figure 9 Results of Ramp $\bar{\sigma}_r$ Input, N = 2.

see errata

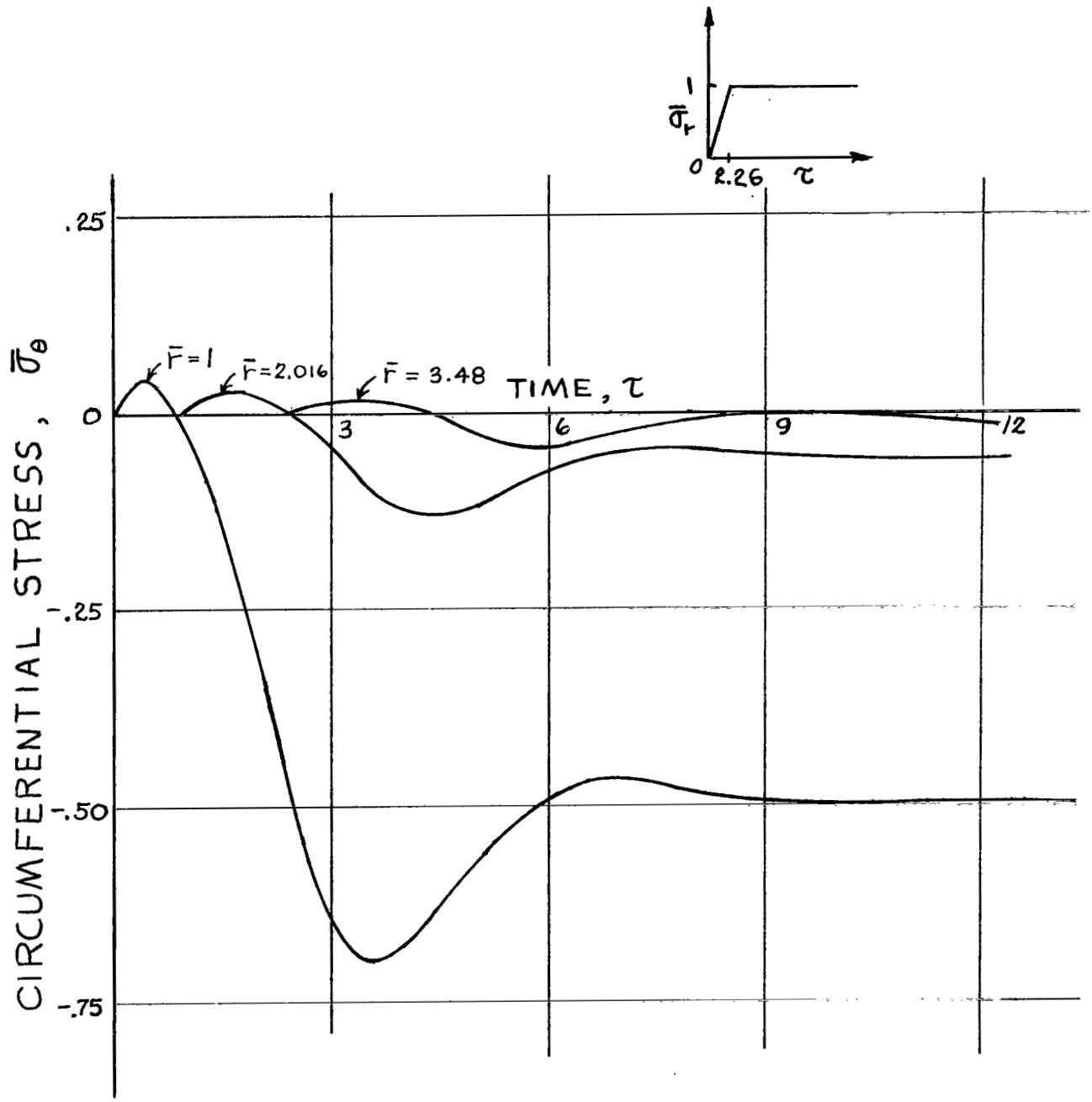

b. Circumferential stress, $\bar{\sigma}_\theta$, versus time, τ.

Figure 9 Results of Ramp $\bar{\sigma}_r$ Input, N = 2.

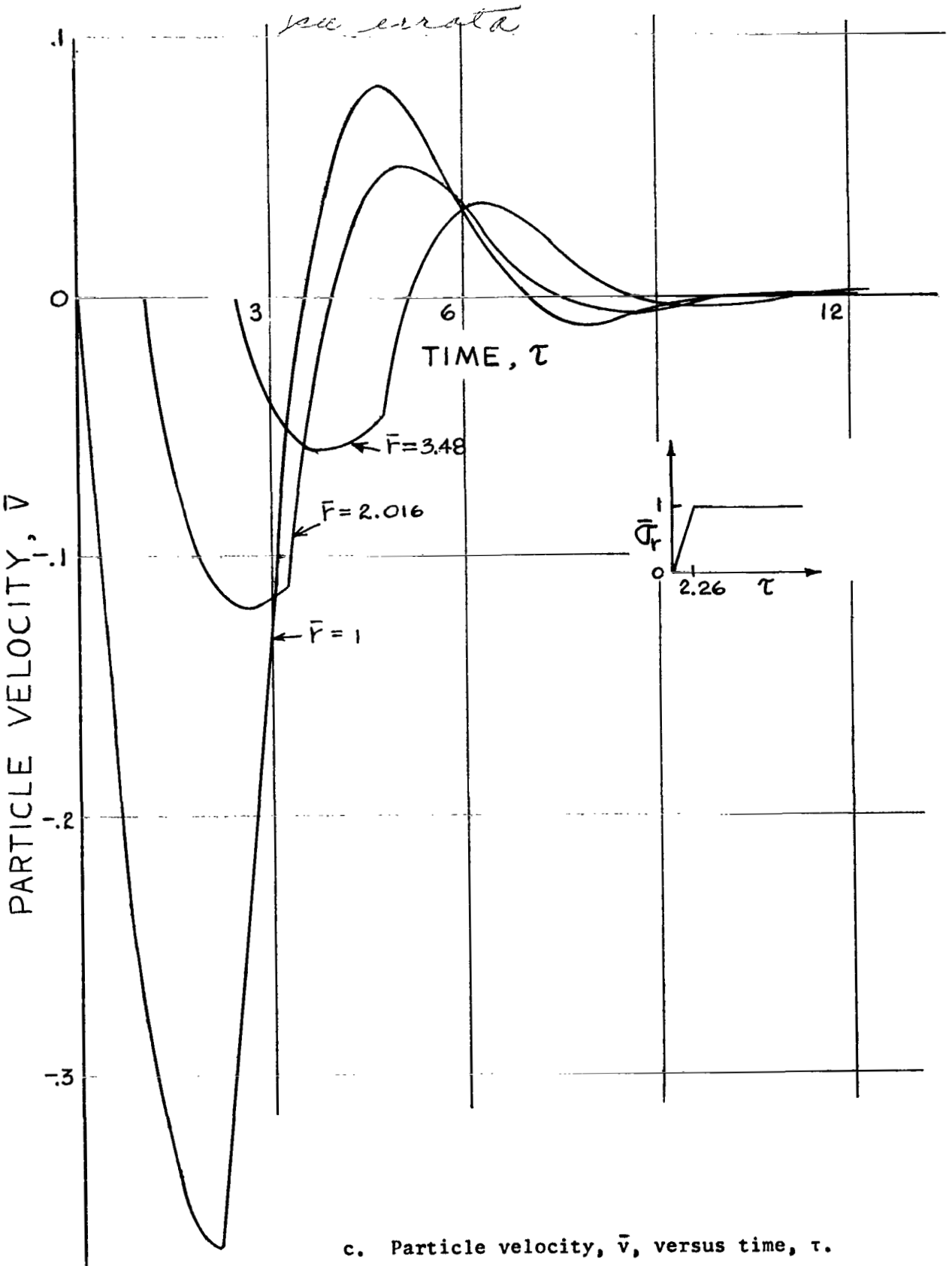

c. Particle velocity, $\bar{v}$, versus time, τ.

Figure 9 Results of Ramp $\bar{\sigma}_r$ Input, N = 2.

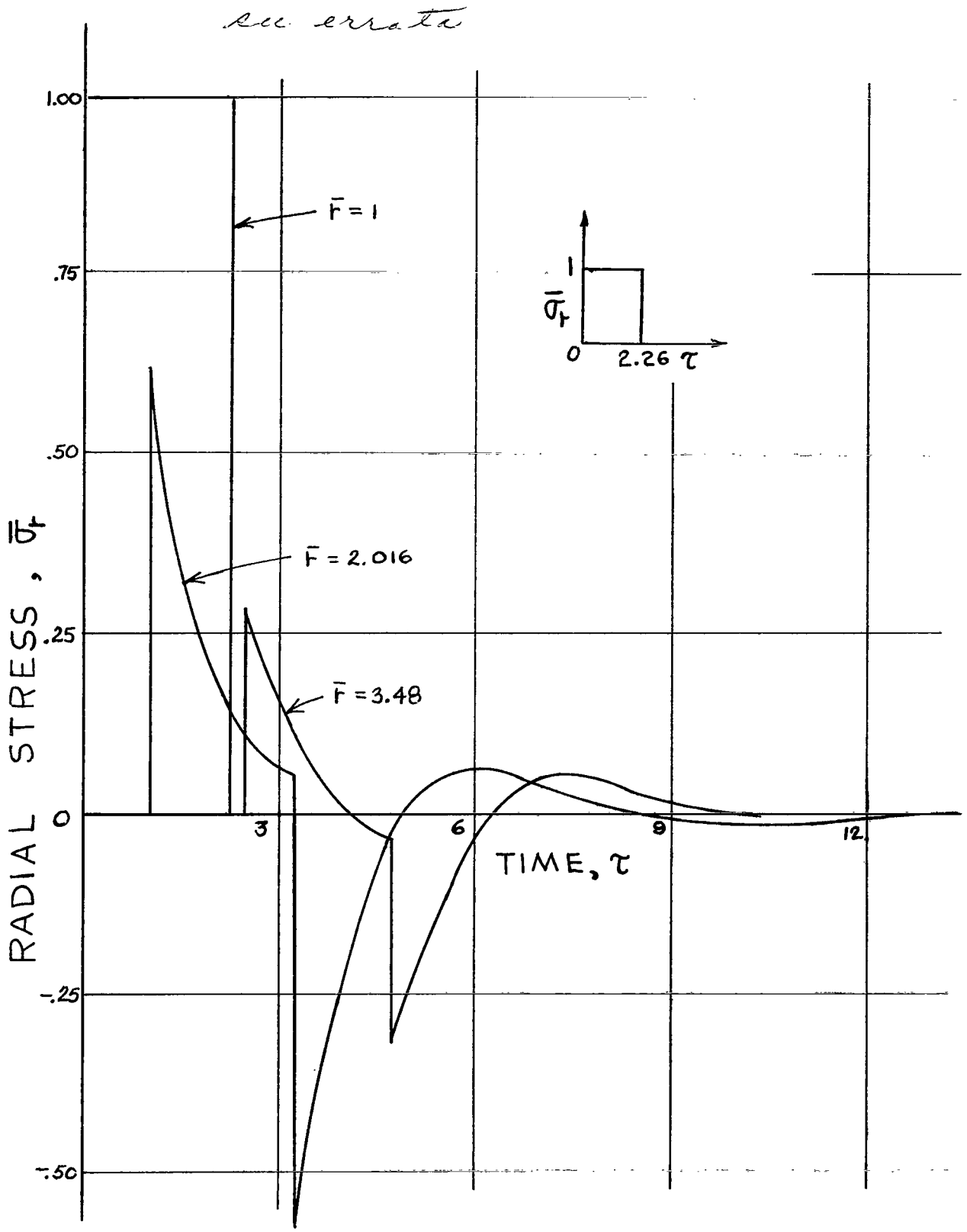

a. Radial stress, $\bar{\sigma}_r$, versus time, τ.

Figure 10 Results of Impulsive $\bar{\sigma}_r$ Input, N = 2.

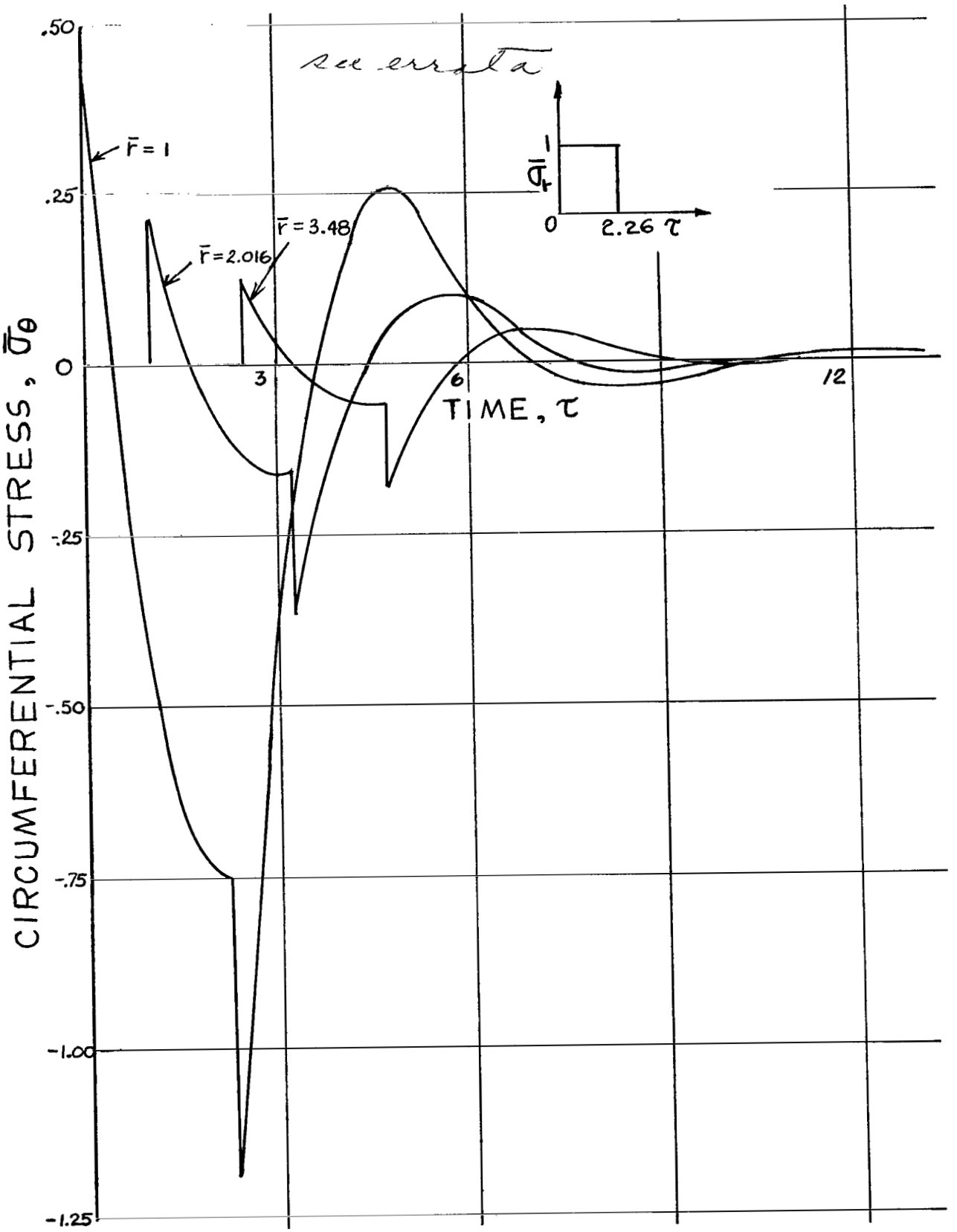

b. Circumferential stress, $\bar{\sigma}_\theta$, versus time, τ.

Figure 10 Results of Impulsive $\bar{\sigma}_r$ Input, N = 2.

all errata

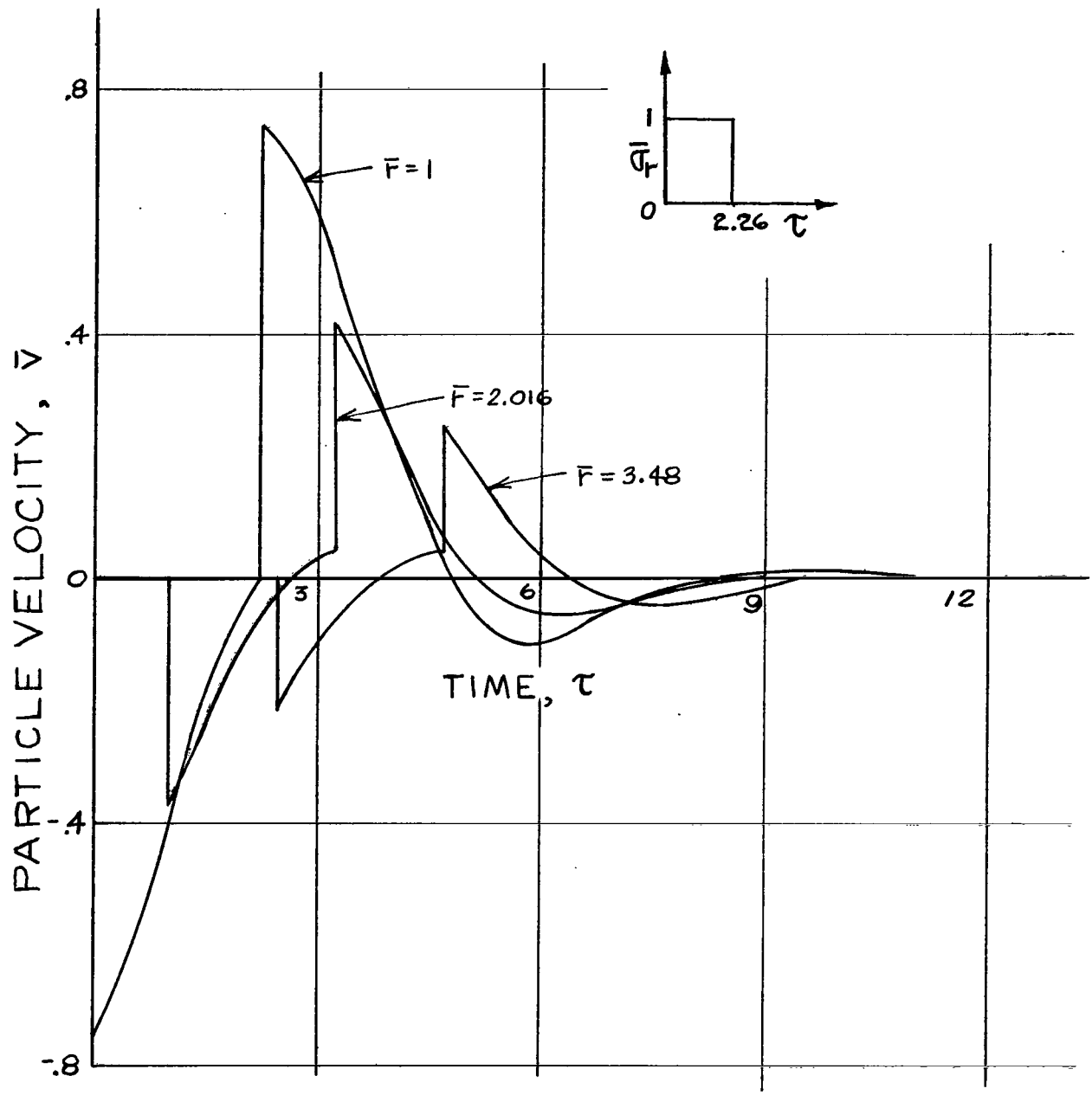

c. Particle velocity, $\bar{v}$, versus time, τ.

Figure 10 Results of Impulsive $\bar{\sigma}_r$ Input, N = 2.

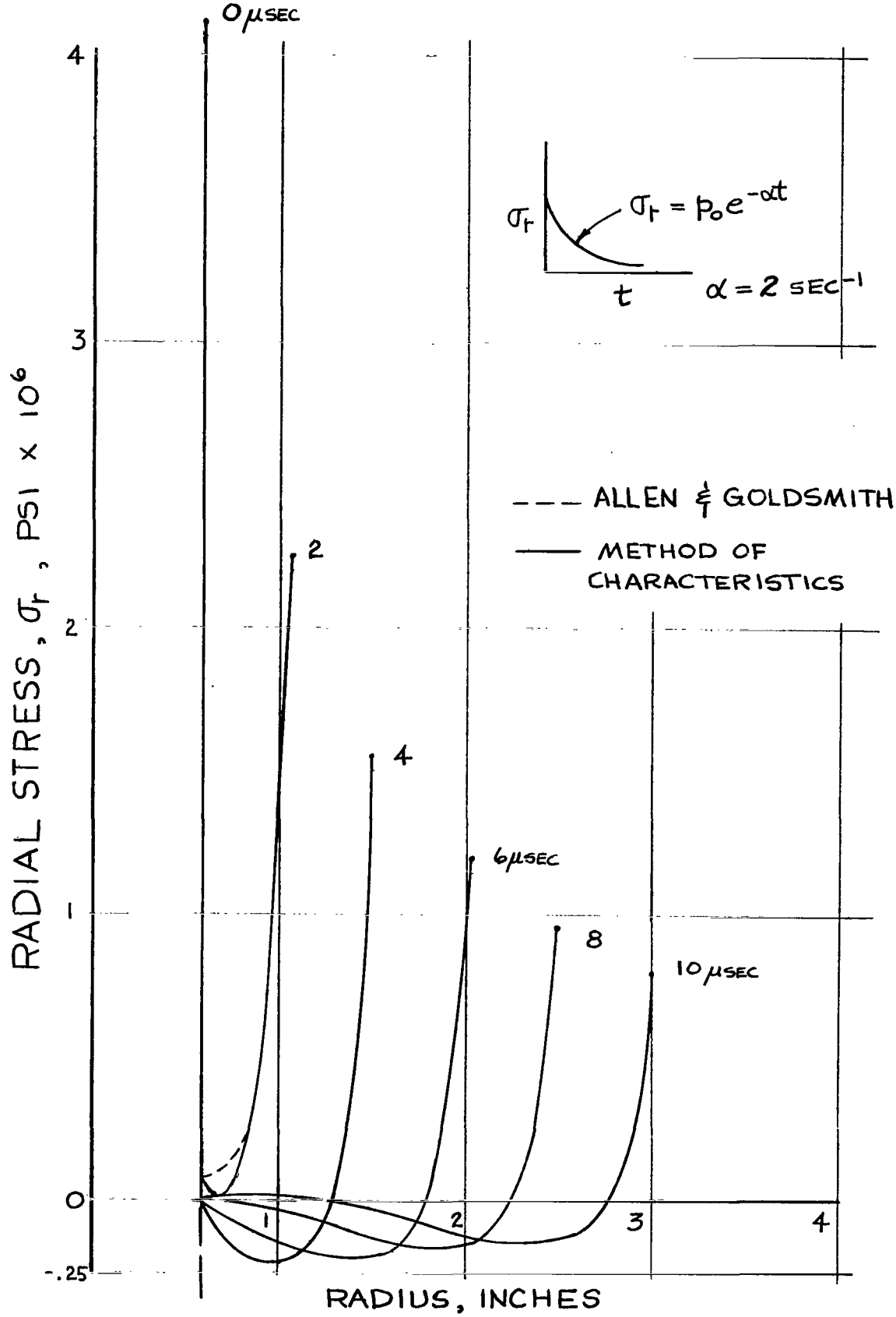

a. Radial stress, σ_r, versus radius r.

Figure 11 Results of Exponential σ_r Input, N = 2.

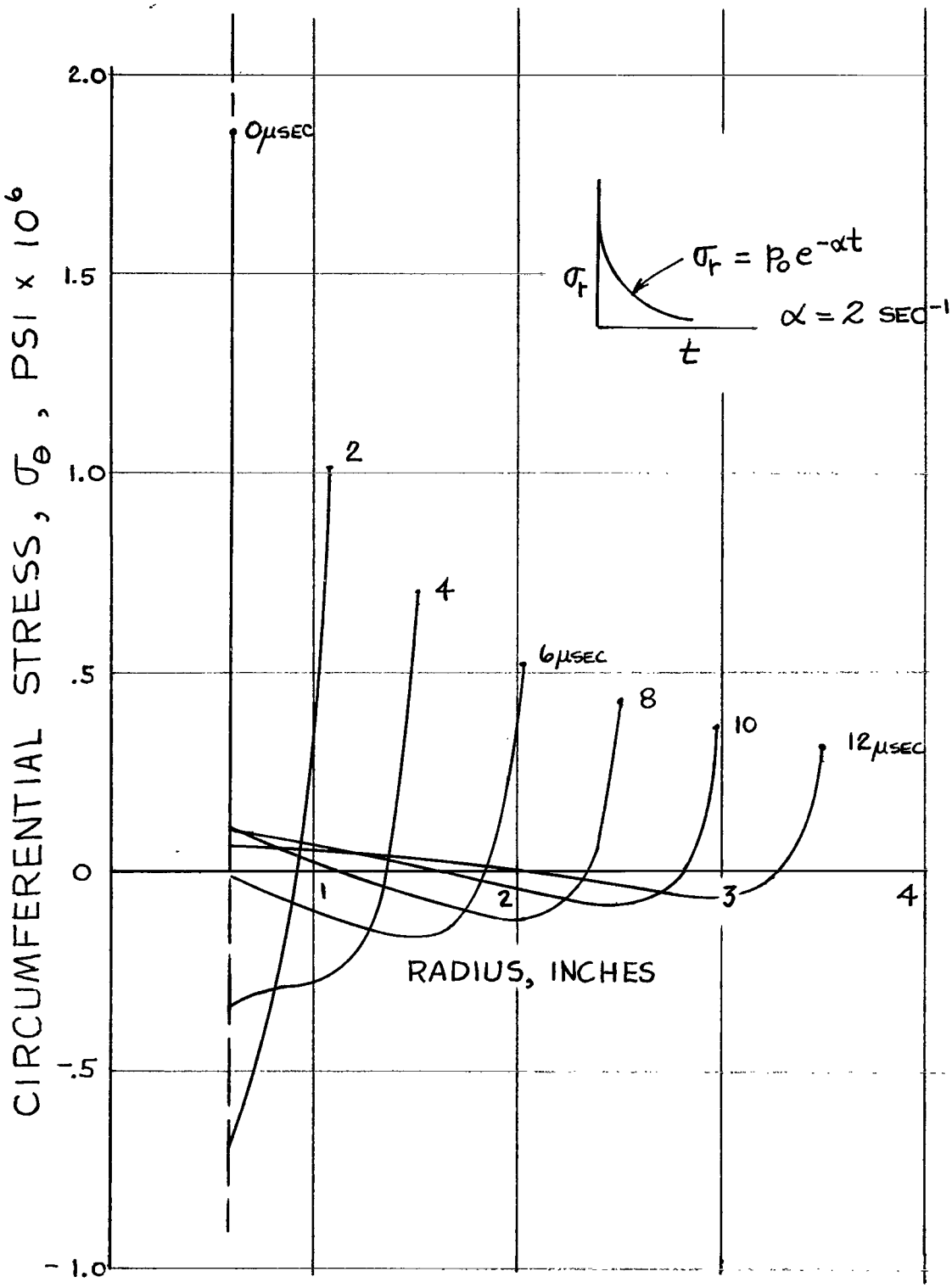

b. Circumferential stress, σ_θ, versus radius r.

Figure 11 Results of Exponential σ_r Input, N = 2.

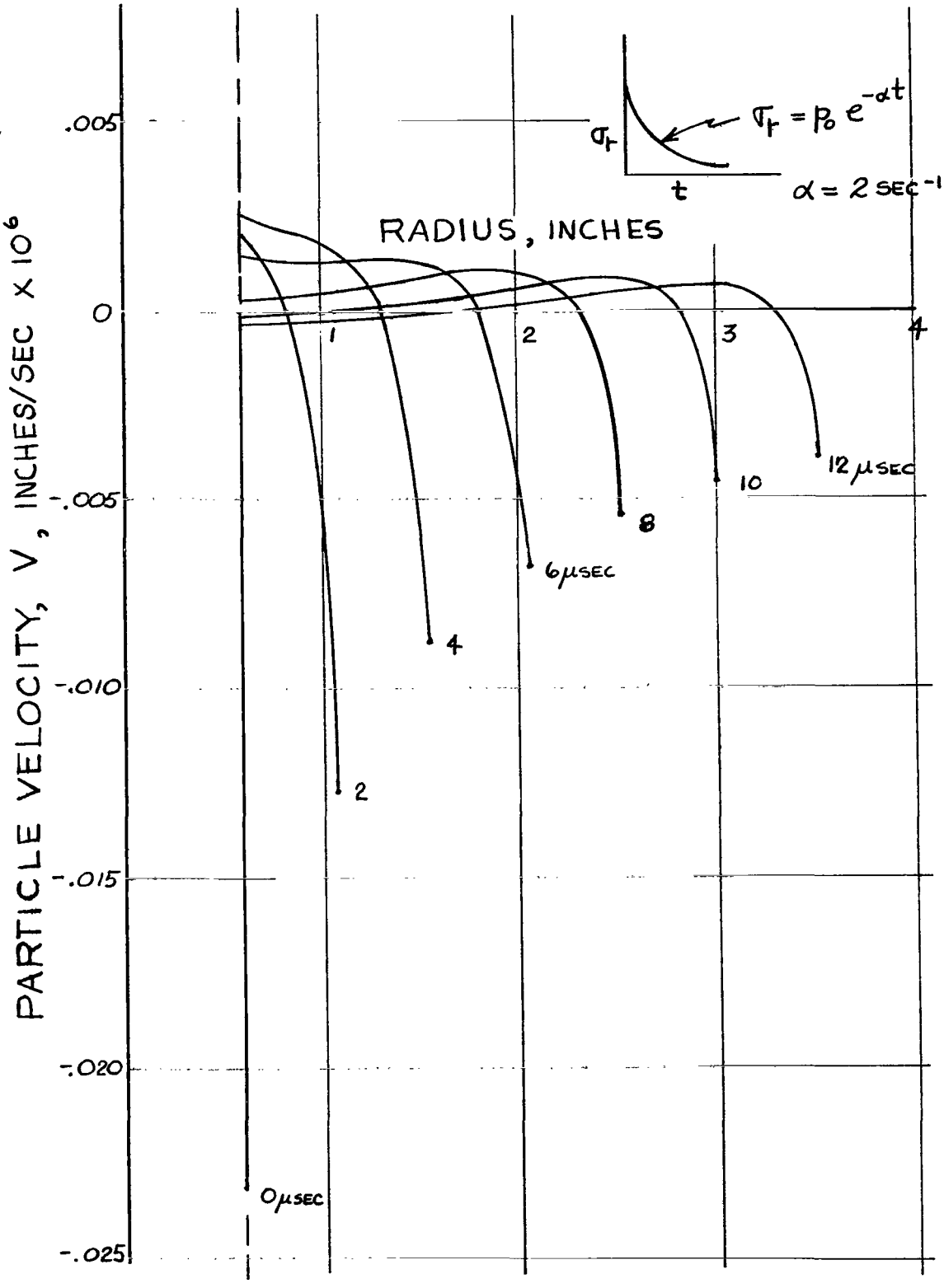

c. Particle velocity, v, versus radius r.

Figure 11 Results of Exponential σ_r Input, N = 2.

APPENDIX A

Derivation of Governing Equations

In this appendix, we shall derive the governing differential equations for the propagation of plane longitudinal waves in bars, sheets, and infinite bodies; the governing equations for cylindrical waves in sheets and axisymmetric bodies; and the governing equations for spherical waves. All these equations will then be represented by one set of generalized equations.

For a plane wave traveling in an elastic medium according to the elementary theory of wave propagation and neglecting the dispersion effect, we have [15]

$$\frac{\partial \sigma_x}{\partial x} = \rho \frac{\partial^2 u}{\partial t^2} \tag{A.1}$$

This is the governing differential equation for plane waves in all three types of body geometry, (i.e., bar, sheet, and infinite body). Hooke's Law, however, for each of these cases is different. For plane waves traveling in an elastic bar, Hooke's Law is given by

$$\frac{\partial u}{\partial x} = \frac{1}{E_o} \sigma_x \tag{A.2}$$

where x is the coordinate along the axis of the bar, σ_x is the normal stress on a plane perpendicular to the axis of bar and u is the displacement in x-direction. Eq. (A.1) is the equation of motion, while (A.2) is Hooke's Law with $\epsilon_x = \partial u/\partial x$.

For a plane wave traveling along the x-direction in a sheet or thin plate, due to the constraint in y-direction, $\sigma_y \neq 0$ but $\varepsilon_y = \sigma_z = 0$.

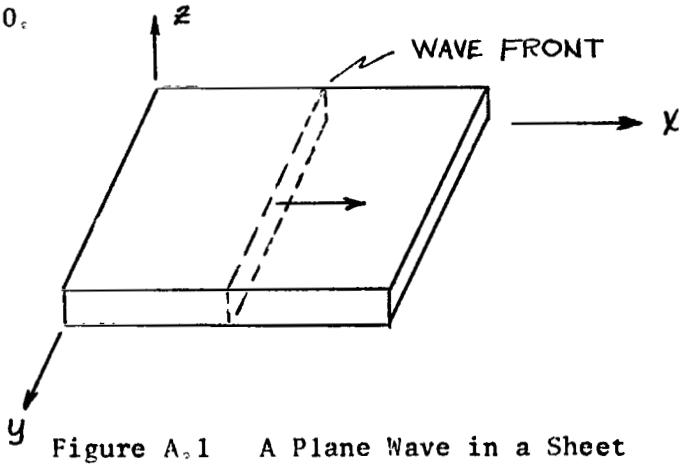

Figure A.1 A Plane Wave in a Sheet

According to the generalized Hooke's Law

$$\epsilon_y = \frac{1}{E_o}\left[\sigma_y - \nu_o(\sigma_x + \sigma_z)\right]$$

or

$$\sigma_y = \nu_o \sigma_x \quad (\text{SINCE} \quad \sigma_z = 0) \tag{A.3}$$

Therefore,

$$\epsilon_x = \frac{\partial u}{\partial x} = \frac{1}{E_o}\left[\sigma_x - \nu_o \sigma_y\right] = \frac{1-\nu_o^2}{E_o}\sigma_x \tag{A.4}$$

For a plane wave traveling along the x-direction in an infinite elastic body, there are restraints in both y and z direction, therefore $\varepsilon_y = \varepsilon_z = 0$ and $\sigma_y = \sigma_z$, or

$$\epsilon_y = \frac{1}{E_o}\left[\sigma_y - \nu_o(\sigma_x + \sigma_z)\right] = 0$$

$$\sigma_y = \sigma_z = \frac{\nu_o}{1-\nu_o}\sigma_x \tag{A.5}$$

The generalized Hooke's Law in the x-direction then gives

$$\epsilon_x = \frac{\partial u}{\partial x} = \frac{1}{E_o}\left[\sigma_x - \nu_o(\sigma_y + \sigma_z)\right] = \frac{1 - \nu_o - 2\nu_o^2}{E_o(1-\nu_o)}\sigma_x \quad (A.6)$$

The stress-strain relations (A.2), (A.4), and (A.6) may be combined into one equation as

$$\frac{\partial u}{\partial x} = \frac{1}{E}\sigma_x \quad (A.7)$$

where

$$E = E_o \quad \text{for the bar} \quad (A.8)$$

$$E = E_1 = \frac{E_o}{1-\nu_o^2} \quad \text{for the sheet} \quad (A.9)$$

$$E = E_2 = \frac{E_o(1-\nu_o)}{1-\nu_o-2\nu_o^2} \quad \text{for the infinite body} \quad (A.10)$$

Eqs. (A.1) and (A.7), then, are the governing equations for plane waves.

For a cylindrical dilatation wave, the equation of motion in plane polar coordinates is

$$\frac{\partial \sigma_r}{\partial r} + \frac{\sigma_r - \sigma_\theta}{r} = \rho\frac{\partial^2 u}{\partial t^2} \quad (A.11)$$

The derivation of this equation can be found in any textbook in static elasticity, with the body force replaced by the inertia force, $-\rho\,\partial^2 u/\partial t$ where u is the radial displacement. Eq. (A.11) is applicable for both a sheet (plane stress) or an infinite cylindrical body (plane strain). The Hooke's law equation, however, assumes different forms. For the sheet, we have $\sigma_z = 0$,

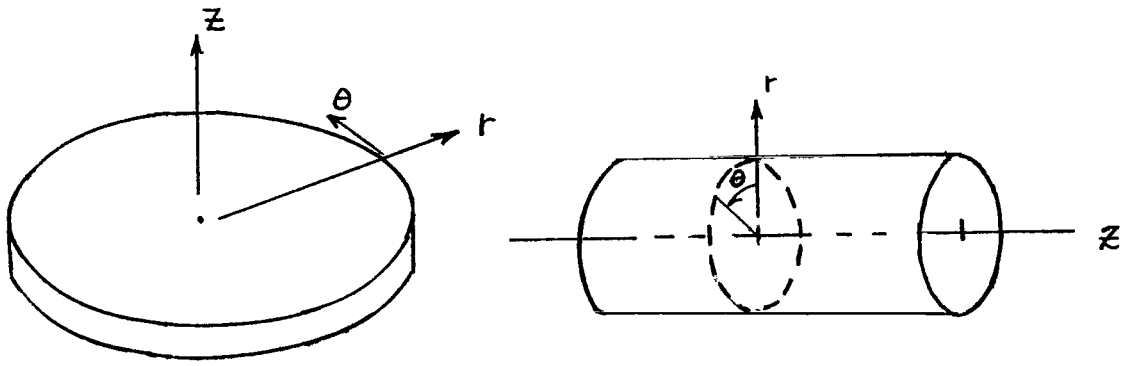

Plane Stress Plane Strain

Figure A.2 Cylindrical Waves in Sheets (plane stress) and in Infinite Body (plane strain)

therefore

$$\epsilon_r = \frac{\partial u}{\partial r} = \frac{1}{E_o}\left(\sigma_r - \nu_o \sigma_\theta\right) \tag{A.12}$$

and

$$\epsilon_\theta = \frac{u}{r} = \frac{1}{E_o}\left(\sigma_\theta - \nu_o \sigma_r\right) \tag{A.13}$$

For the infinite cylindrical body, $\epsilon_z = 0$, thus we have

$$\epsilon_z = \frac{1}{E_o}\left[\sigma_z - \nu_o\left(\sigma_r + \sigma_\theta\right)\right]$$
$$\sigma_z = \nu_o\left(\sigma_r + \sigma_\theta\right) \tag{A.14}$$

Therefore,

$$\epsilon_r = \frac{\partial u}{\partial r} = \frac{1}{E_o}\left[\sigma_r - \nu_o\left(\sigma_\theta + \sigma_z\right)\right]$$
$$= \frac{1-\nu_o^2}{E_o}\left(\sigma_r - \frac{\nu_o}{1-\nu_o}\sigma_\theta\right) \tag{A.15}$$

and

$$\epsilon_\theta = \frac{u}{r} = \frac{1}{E_o}\left[\sigma_\theta - \nu_o\left(\sigma_r + \sigma_z\right)\right] = \frac{1-\nu_o^2}{E_o}\left(\sigma_\theta - \frac{\nu_o}{1-\nu_o}\sigma_r\right) \tag{A.16}$$

Eqs. (A.12), (A.13), (A.15), and (A.16) may be represented by two equations

$$\frac{\partial u}{\partial r} = \frac{1}{E}\left(\sigma_r - \nu\,\sigma_\theta\right) \tag{A.17}$$

$$\frac{u}{r} = \frac{1}{E}\left(\sigma_\theta - \nu\,\sigma_r\right) \tag{A.18}$$

where

$$\left.\begin{aligned} E &= E_o \\ \nu &= \nu_o \end{aligned}\right\} \quad \text{for sheets} \tag{A.19}$$

$$\left.\begin{aligned} E = E_1 &= \frac{E_o}{1-\nu_o^2} \\ \nu = \nu_1 &= \frac{\nu_o}{1-\nu_o} \end{aligned}\right\} \quad \text{for infinite cylindrical body} \tag{A.20}$$

For a spherical dilatation wave involving only radial displacement, the equation of motion is

$$\frac{\partial \sigma_r}{\partial r} + \frac{2(\sigma_r - \sigma_\theta)}{r} = \rho\,\frac{\partial^2 u}{\partial t^2} \tag{A.21}$$

This type of wave can only exist in an infinite body. The normal stresses in the two directions orthogonal to r, due to symmetry, must be equal, or $\sigma_\theta = \sigma_\phi$, therefore

$$\epsilon_r = \frac{\partial u}{\partial r} = \frac{1}{E_o}\left[\sigma_r - \nu_o\left(\sigma_\theta + \sigma_\phi\right)\right] = \frac{1}{E_o}\left(\sigma_r - 2\nu_o\,\sigma_\theta\right) \tag{A.22}$$

$$\epsilon_\theta = \frac{2u}{r} = \frac{1}{E_o}\left[\sigma_\theta - \nu_o\left(\sigma_r + \sigma_\phi\right)\right] = \frac{1}{E_o}\left[\sigma_\theta(1-\nu_o) - \nu_o\,\sigma_r\right] \tag{A.23}$$

see errata

All of the previously derived governing differential equations may be consolidated into one set of equations, with r as the direction of wave propagation,

$$\frac{\partial \sigma_r}{\partial r} + \frac{N(\sigma_r - \sigma_\theta)}{r} = \rho \frac{\partial^2 u}{\partial t^2} \tag{A.24}$$

$$\frac{\partial u}{\partial r} = \frac{1}{E}\left(\sigma_r - N\nu\sigma_\theta\right) \tag{A.25}$$

$$N\frac{u}{r} = N\frac{1}{E}\left\{\sigma_\theta\left[1 - (N-1)\nu\right] - \nu\sigma_r\right\} \tag{A.26}$$

where N, E, and ν are constants, assuming different values according to the rule:

$N = 0$ (plane waves)

$E = E_o$ in bar

$E = E_1$ in sheet

$E = E_2$ in infinite body

$N = 1$ (cylindrical waves)

$E = E_o$, $\nu = \nu_o$ } in sheet

$E = E_1$, $\nu = \nu_1$ } in infinite cylindrical body

$N = 2$ (spherical waves)

$E = E_o$

$\nu = \nu_o$

It should be noted that for the plane waves in bars and in sheets, as well as the cylindrical waves in sheets, the governing equations are approximate in nature, as discussed in any standard text in elasticity. For the cases of plane, cylindrical and spherical waves in an infinite body, these equations are exact.

Combining eqs. (A.24), (A.25), and (A.26), and eliminating σ_r and σ_θ, we have

$$\frac{\partial^2 u}{\partial r^2} + N \frac{\partial}{\partial r}\left(\frac{u}{r}\right) = \frac{1}{c^2} \frac{\partial^2 u}{\partial t^2} \tag{A.27}$$

where

$$c = \left[\frac{E}{\rho} \frac{[1 - (N-1)\nu]}{[1 - (N-1)\nu - N\nu^2]}\right]^{\frac{1}{2}} \tag{A.28}$$

is the velocity of wave propagation. For plane waves (N = 0),

in bars: $$c = c_o = \sqrt{\frac{E_o}{\rho}} = \text{bar velocity} \tag{A.29}$$

in sheets: $$c = c_p = \sqrt{\frac{E_1}{\rho}} = \sqrt{\frac{E_o}{\rho(1-\nu_o^2)}} = \text{plate velocity} \tag{A.30}$$

in infinite bodies: $$c = c_2 = \sqrt{\frac{E_2}{\rho}} = \sqrt{\frac{E_o(1-\nu_o^2)}{\rho(1-\nu_o-2\nu_o^2)}} = \text{dilatation velocity} \tag{A.31}$$

For cylindrical waves (N = 1)

in sheets: $$c = c_p = \sqrt{\frac{E_o}{\rho(1-\nu_o^2)}} = \text{plate velocity} \tag{A.32}$$

in infinite bodies: $$c = c_2 = \sqrt{\frac{E_1}{\rho(1-\nu_1^2)}} = \sqrt{\frac{E_o(1-\nu_o)}{\rho(1-\nu_o-2\nu_o^2)}} = \text{dilatation velocity} \tag{A.33}$$

For spherical waves (N = 2)

$$c = c_2 = \sqrt{\frac{E_o(1-\nu_o)}{\rho(1-\nu_o-2\nu_o^2)}} = \text{dilatation velocity} \tag{A.34}$$

From these equations, it may be seen that in bars, plane waves travel at the bar velocity; in sheets, both plane and cylindrical waves travel at the plate velocity; while in infinite bodies, all waves (plane, cylindrical and spherical) travel at the dilatation velocity. These results are summarized in Table A.1.

TABLE A.1

Constants for Different Cases

N		Bar	Sheet	Infinite Body
0	E	E_o	E_1	E_2
	ν	—	—	—
	c	c_o	c_p	c_2
1	E	—	E_o	E_1
	ν	—	ν_o	ν_1
	c	—	c_p	c_2
2	E	—	—	E_o
	ν	—	—	ν_o
	c	—	—	c_2

APPENDIX B

Method of Characteristics (For general reference, see [14].)

In this appendix, the method of characteristics as applied to the system of eqs. (14), (15), and (16) is outlined for reference. We consider in this discussion only regions in the physical plane (r,t-plane) where the stresses and velocity are continuous. Hence we may write

$$\begin{aligned} d\sigma_r &= \frac{\partial \sigma_r}{\partial r} dr + \frac{\partial \sigma_r}{\partial t} dt \\ d\sigma_\theta &= \frac{\partial \sigma_\theta}{\partial r} dr + \frac{\partial \sigma_\theta}{\partial t} dt \\ dv &= \frac{\partial v}{\partial r} dr + \frac{\partial v}{\partial t} dt \end{aligned} \tag{B.1}$$

We shall seek curves in the r,t-plane along which the derivatives of σ_r, σ_θ, and v might be discontinuous. Such curves, when they exist, shall be called the physical characteristics. Discontinuity in the derivatives of σ_r, σ_θ, and v implies that $\partial\sigma_r/\partial r$, $\partial\sigma_r/\partial t$, $\partial\sigma_\theta/\partial r$, $\partial\sigma_\theta/\partial t$, $\partial v/\partial r$, and $\partial v/\partial t$ are indeterminate along the physical characteristics. If these six derivatives are considered as unknown variables, they are related by the six eqs. (14), (15), (16), and (B.1) as follows:

$$\begin{aligned}
r\frac{\partial \sigma_r}{\partial r} \qquad\qquad & -\rho r \frac{\partial v}{\partial t} = N(\sigma_\theta - \sigma_r) \\
-\frac{1}{E}\frac{\partial \sigma_r}{\partial t} \qquad & +\frac{N\nu}{E}\frac{\partial \sigma_\theta}{\partial t} + \frac{\partial v}{\partial r} = 0 \\
+\frac{\nu}{E}\frac{\partial \sigma_r}{\partial t} \qquad & -\frac{M}{E}\frac{\partial \sigma_\theta}{\partial t} = -\frac{v}{r} \\
dr\frac{\partial \sigma_r}{\partial r} + dt\frac{\partial \sigma_r}{\partial t} \qquad\qquad & = d\sigma_r \\
dr\frac{\partial \sigma_\theta}{\partial r} + dt\frac{\partial \sigma_\theta}{\partial t} \qquad\qquad & = d\sigma_\theta \\
dr\frac{\partial v}{\partial r} + dt\frac{\partial v}{\partial t} \qquad\qquad & = dv
\end{aligned} \tag{B.2}$$

where $M = [1 - (N - 1)\nu]$. Solving these equations for $\partial\sigma_r/\partial r$, we have

$$\frac{\partial \sigma_r}{\partial r} = \frac{\begin{vmatrix} N(\sigma_\theta - \sigma_r) & 0 & 0 & 0 & 0 & -\rho r \\ 0 & -1/E & 0 & N\nu/E & 1 & 0 \\ -\nu/r & \nu/E & 0 & -M/E & 0 & 0 \\ d\sigma_r & dt & 0 & 0 & 0 & 0 \\ d\sigma_\theta & 0 & dr & dt & 0 & 0 \\ dv & 0 & 0 & 0 & dr & dt \end{vmatrix}}{\begin{vmatrix} r & 0 & 0 & 0 & 0 & -\rho r \\ 0 & -1/E & 0 & N\nu/E & 1 & 0 \\ 0 & \nu/E & 0 & -M/E & 0 & 0 \\ dr & dt & 0 & 0 & 0 & 0 \\ 0 & 0 & dr & dt & 0 & 0 \\ 0 & 0 & 0 & 0 & dr & dt \end{vmatrix}}$$

$$= \frac{1}{\frac{1}{E}(dr)^3\left(\frac{dt}{dr} + \frac{1}{c}\right)\left(\frac{dt}{dr} - \frac{1}{c}\right)} \cdot \left\langle \frac{1}{E}(dr)^2 \left\{ M\frac{dt}{dr}\left[N(\sigma_\theta - \sigma_r)dt + \rho r dv\right] - \rho r\left[\frac{1}{E}d\sigma_r(M - N\nu^2) - N\nu\frac{v}{r}dt\right]\right\}\right\rangle \tag{B.3}$$

This derivative is indeterminate if both the numerator and denominator are equal to zero. The vanishing of the denominator yields three physical characteristics,

$$\begin{aligned} I^+ \text{ char.} \quad & \frac{dr}{dt} = +c \\ I^- \text{ char.} \quad & \frac{dr}{dt} = -c \\ II \text{ char.} \quad & dr = 0 \end{aligned} \tag{B.4}$$

For $dr/dt = \pm c$, the vanishing of the numerator of (B.3) yields the characteristic equations, which govern the variables σ_r, σ_θ, and v along I^+ and I^- physical characteristics. These equations

are, along $dr/dt = \pm c$,

$$d\sigma_r \mp \rho c\, dv = \left\{ -N(\sigma_r - \sigma_\theta) \pm \rho \nu c \sqrt{\left[\frac{N}{1-(N-1)\nu}\right]} \right\} \frac{dr}{r} \qquad \text{(B.5)}$$

From eq. (B.3), the characteristic equation along the physical characteristic $dr = 0$ cannot be obtained, since $(dr)^2$ also appears in the numerator as a common factor. Solving the system of eqs. (B.2) for $\partial\sigma_r/\partial t$, $\partial\sigma_\theta/\partial t$, $\partial v/\partial r$, or $\partial v/\partial t$ gives the same result as eq. (B.3), i.e., it yields the same three physical characteristics I^+, I^-, II, and the same characteristic eqs. (B.5) along I^+ and I^-. Solving for $\partial\sigma_\theta/\partial r$, however, we obtain a different result.

$$\frac{d\sigma_\theta}{dr} = \frac{1}{\frac{1}{E}(dr)^3\left(\frac{dt}{dr}+\frac{1}{c}\right)\left(\frac{dt}{dr}-\frac{1}{c}\right)} \left\{ -r\left[\frac{\nu}{E}d\sigma_r - \frac{M}{E}d\sigma_\theta + \frac{v}{r}dt\right] + \frac{\nu}{E}\left(\frac{dr}{dt}\right)\left[N(\sigma_\theta - \sigma_r)\,dt + \rho r\, dv\right] + \rho r\left(\frac{dr}{dt}\right)^2 \left[\frac{v}{Er}dt + N\left(\frac{\nu}{E}\right)^2 d\sigma_\theta - \frac{M}{E^2}d\sigma_\theta\right] \right\} \qquad \text{(B.6)}$$

The vanishing of the denominator gives the same three physical characteristics I^+, I^-, and II as previously derived. The vanishing of the numerator with $dr/dt = \pm c$ yields the characteristic eqs. (B.5). In addition, the vanishing of the numerator with $dr = 0$ produces the characteristic equation along II, i.e.,

$$\frac{d\sigma_r}{d\sigma_\theta} = \left\{ \left[1-(N-1)\nu\right] - \frac{Ev}{r}\frac{dt}{d\sigma_\theta} \right\} \frac{1}{\nu} \qquad \text{(B.7)}$$

"The aeronautical and space activities of the United States shall be conducted so as to contribute . . . to the expansion of human knowledge of phenomena in the atmosphere and space. The Administration shall provide for the widest practicable and appropriate dissemination of information concerning its activities and the results thereof."

—NATIONAL AERONAUTICS AND SPACE ACT OF 1958

NASA SCIENTIFIC AND TECHNICAL PUBLICATIONS

TECHNICAL REPORTS: Scientific and technical information considered important, complete, and a lasting contribution to existing knowledge.

TECHNICAL NOTES: Information less broad in scope but nevertheless of importance as a contribution to existing knowledge.

TECHNICAL MEMORANDUMS: Information receiving limited distribution because of preliminary data, security classification, or other reasons.

CONTRACTOR REPORTS: Technical information generated in connection with a NASA contract or grant and released under NASA auspices.

TECHNICAL TRANSLATIONS: Information published in a foreign language considered to merit NASA distribution in English.

TECHNICAL REPRINTS: Information derived from NASA activities and initially published in the form of journal articles.

SPECIAL PUBLICATIONS: Information derived from or of value to NASA activities but not necessarily reporting the results of individual NASA-programmed scientific efforts. Publications include conference proceedings, monographs, data compilations, handbooks, sourcebooks, and special bibliographies.

Details on the availability of these publications may be obtained from:

SCIENTIFIC AND TECHNICAL INFORMATION DIVISION

NATIONAL AERONAUTICS AND SPACE ADMINISTRATION

Washington, D.C. 20546